

CRITICAL REVIEW

[View Article Online](#)  
[View Journal](#) | [View Issue](#)



Cite this: *RSC Sustainability*, 2025, **3**, 2501

## Sustainable and durable superwetting textiles coated with polydopamine for oil/water separation

Abdul Kalam Azad,<sup>a</sup> Nedal Y. Abu-Thabit <sup>\*a</sup> and Mahmoud H. Abu Elella<sup>b</sup>

The industrial revolution and the frequent crude oil spills have caused tremendous contamination of the natural water resources with oily waste. Superwetting textiles have been proposed as advanced functional materials for selective oil separation from oily wastewater. Superwetting textiles have been fabricated by engineering smart coatings that allow for the modified textile's optimal surface roughness and chemical composition. During the past decade, polydopamine (PDA) has been proposed as a sustainable, biodegradable, and biomimetic coating for the fabrication of superwetting textiles with superhydrophobic and/or underwater superoleophobic properties. PDA coatings offer advantages including a simple coating procedure in a wide pH range, use of various organic/inorganic oxidants, high adhesion strength to various substrates, increased surface roughness of the coated substrates, and diverse post-functionalization *via* different ionic/covalent interactions. Thus, bioinspired, sustainable and durable superwetting textiles have been designed and fabricated by controlling the surface roughness and the surface energy of the PDA-coated textiles. This review highlights the recent advances in fabricating superwetting PDA-coated textiles for the separation of various oil/water mixtures. Two classes of superwetting textiles are discussed, including superhydrophobic (SHB) and superhydrophilic/underwater superoleophobic (SHL/UWSOB) PDA-coated textiles. In each case, the discussion focuses on the fabrication methods, coating procedures, separation performance, recyclability, and enhanced mechanical and chemical durability due to the synergistic effect of the deposited and/or functionalized PDA coating. The discussion includes the separation of emulsified mixtures, current challenges, proposed solutions, and future perspectives of PDA-coated textiles for practical and large-scale oil/water separations.

Received 19th January 2025  
Accepted 20th April 2025

DOI: 10.1039/d5su00041f  
[rsc.li/rscsus](http://rsc.li/rscsus)

### Sustainability spotlight

During the past two decades, developing superwetting materials has emerged as an advanced technology for the efficient separation of oil/water mixtures. Among various special wettability materials, textiles and fabrics have been proposed as flexible porous membranes for the treatment of oily wastewater and crude oil spills. Superwetting textiles modified with polydopamine (PDA) coatings are regarded as a sustainable class of smart multifunctional materials for the treatment of stratified and emulsified oil/water mixtures. PDA coatings offer advantages such as low cost, versatility, biodegradability, and simple fabrication that avoids the use of harsh chemicals/conditions. The PDA coating plays a critical role in the fabrication of durable superwetting textiles by enhancing the adhesion and surface roughness and offering diverse post-functionalization with low/high surface energy materials.

## 1. Introduction

The industrial revolution has led to increased consumption of freshwater and produced significant oily wastewater by discharging oily waste into various water streams.<sup>1–6</sup> In a similar scenario, frequent crude oil spills have discharged vast quantities of toxic liquid hydrocarbons into the sea or coastal areas, resulting in significant environmental pollution and posing a direct threat to aquatic systems and an indirect risk to public

health and communities.<sup>7–10</sup> Oil can be separated from oily wastewater using traditional methods, including gravity filtration, chemical precipitation, flocculation, coagulation, centrifugation, or thermal incineration.<sup>11–15</sup> However, these methods suffer from low separation efficiency, large footprint requirements, high operation cost, and/or generation of secondary pollution.<sup>16</sup> Therefore, there is a crucial need to develop new and cost-effective materials for efficient separation of oil/water mixtures.

Special wettability materials have superhydrophobic or superhydrophilic superwetting surfaces for liquids on liquid/air/solid or water/oil/solid interfaces with a water contact angle (WCA) greater than 150° or less than 10°, respectively.<sup>17,18</sup> During the past two decades, special wettability materials with

<sup>a</sup>Chemical Engineering Department, Jubail Industrial College, P.O. BOX: 10099, Jubail Industrial City 31961, Saudi Arabia. E-mail: abuthabit\_nidal@yahoo.com; Tel: +966 13 340 5400

<sup>b</sup>Chemistry Department, Faculty of Science, Cairo University, Giza 12613, Egypt



superhydrophobic (SHB) or superhydrophilic and underwater superoleophobic (SHL/UWSOB) surfaces have been proposed as advanced functional materials for the separation of emulsified and stratified oil/water mixtures.<sup>19–21</sup> Typically, the construction of superwetting surfaces can be achieved by tuning the surface roughness and surface energy.<sup>22,23</sup> The common substrates that have been modified as superwetting materials for oil/water separation include fabrics and textiles,<sup>24–26</sup> sponges,<sup>27–30</sup> metal

meshes,<sup>31–34</sup> and polymeric membranes.<sup>35–38</sup> Compared to other substrates, woven and nonwoven textiles have been proposed for efficient separation of oil/water mixtures in harsh environments due to their low cost, high porosity, high permeability, high flexibility, good mechanical durability, and corrosion resistance.<sup>39,40</sup> Unlike superwetting sponges, which have been mainly employed as absorption materials for oil/water separation,<sup>27</sup> superwetting textiles have been utilized as filter

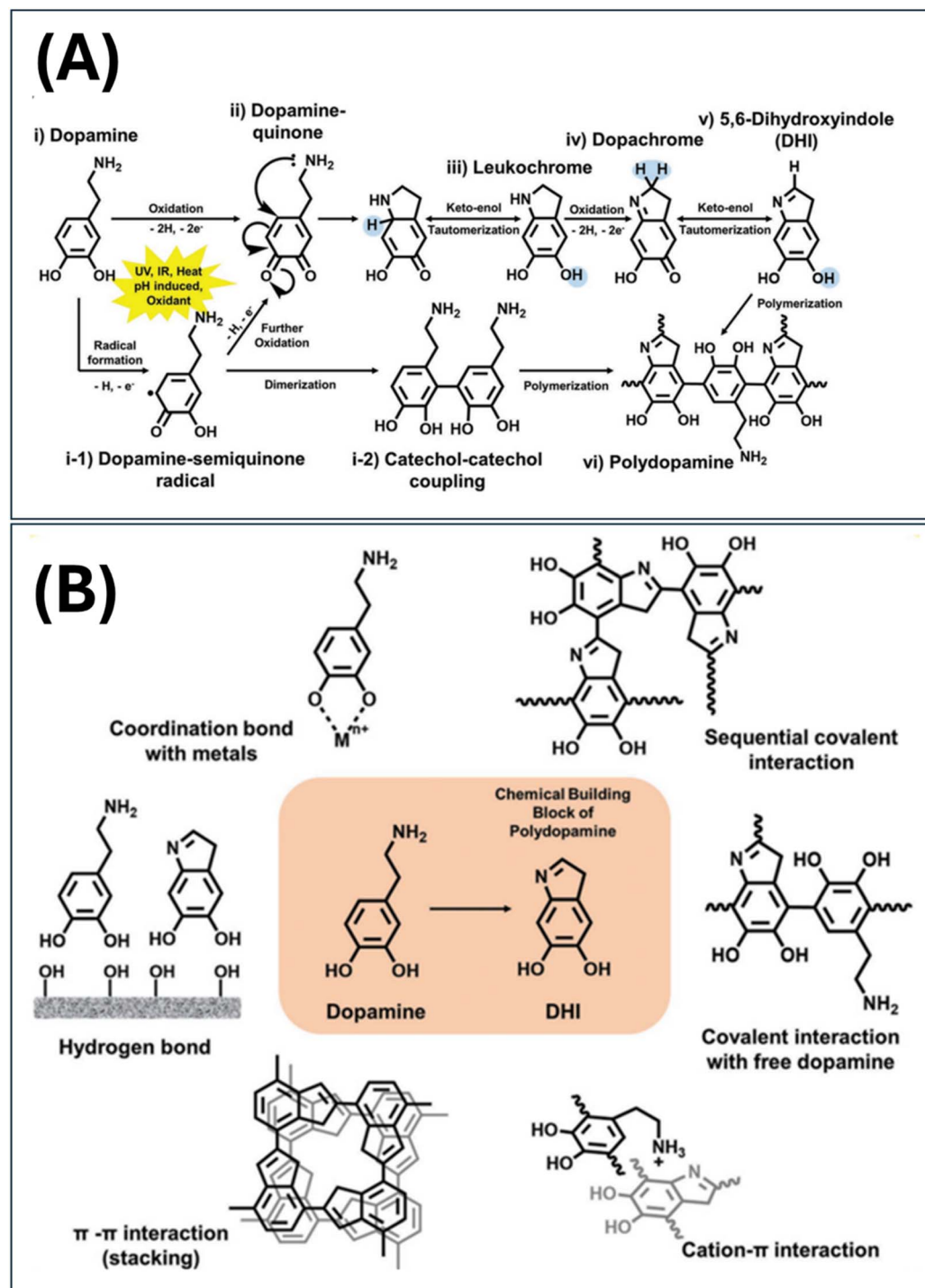


Fig. 1 Polymerization and interaction mechanisms of dopamine. (A) Polydopamine formation: the copolymer consisting of 5,6-dihydroxyindole (DHI) and dopamine. (B) Diverse interactions of dopamine and DHI.<sup>64</sup>



Table 1 PDA-coated superhydrophobic/superoiphilic textiles for oil/water separation<sup>a</sup>

Type of fabric/ textile	Modification materials		Optimum coating parameters				Highest oil permeation Separation efficiency(%)				Ref.
	Surface roughness	Surface energy	DA conc. (mg mL <sup>-1</sup> )	Buffer	Time (h)	Temp. (°C)	Other materials	flux (L m <sup>-2</sup> h <sup>-1</sup> )	(recyclability)	Durability features	
PET	PDA NPs	PFDTs	2	T/P	20	35	—	—	—	*Resistance to abrasion and UV radiation	68
Blended fabric (35% cotton, 65% polyester)	PDA NPs	ODA	1	T-HCl	24	60	Folic acid as SDA	—	97.1	*Resistance to wear and NaCl solution (3.5 wt%)	69
Cotton fabric, polyester gloves	PDA	ODA or ODT	0.5	T-HCl	12	R. T.	—	—	—	*Mechanically induced self- healing superhydrophobicity	70
Cotton	PDA NPs	—	10 mM	T-HCl	24	R. T.	CuSO <sub>4</sub>	—	—	*Resistance to stretching, compression, friction and mechanical washing	71
Cotton fabric	PDA NPs	—	0.02 g	TEOS- HCl/ HMDS	24	q	SiO <sub>2</sub>	4000	99.9	*Durable antibacterial and sticky superhydrophobic properties	72
Cotton, polyester, wool fabric	PDA, polyesters, PDA NPs	HDMTMS	0.1 g/10 mL	—	50	12	—	—	—	*Excellent mechanical stability	72
Cotton	PDA NPs/PEI	—	60 mg mL <sup>-1</sup>	T-HCl	35	14	Borax, TA	—	>98	*Resistance to abrasion and degradation	74
Tetra-copolyester and polypropylene	PDA NPs	PFDT	2	T-HCl	25	12	SiO <sub>2</sub> , AgNO <sub>3</sub>	—	>90	*Resistance to abrasion and washing	73
Cotton fabric	PDA NPs	ODA	2	Sodium perborate (PBS)	90	50	FeCl <sub>3</sub>	—	>96	*Flame retardant and self- extinguishing ability	75
Polylactic acid non-woven fabric	PDA NPs	(PVDF-HFP)	2	T-HCl	20	R. T.	FeCl <sub>2</sub> , 4H <sub>2</sub> O, FeCl <sub>3</sub> , 6H <sub>2</sub> O	—	99.5	*Excellent recyclability and higher absorption capacity	77



Table 1 (Cont'd.)

Type of fabric/ textile	Modification materials		Optimum coating parameters				Highest oil permeation Separation efficiency (%) (recyclability)	Durability features	Ref.
	Surface roughness	Surface energy	DA conc. (mg mL <sup>-1</sup> )	Buffer	Time (h)	Temp. (°C)	Other materials		
Blended fabric (35% cotton, 65% polyester)	PDA NPs	ODT	8	—	4	2.5	Sodium periodate	4500	>97
Blended fabric (50% nylon 56 and 50% cotton)	PDA NPs	DMPA, POSS	0.3 g	T & T-HCl	24	45	MPMDS	—	—
PET, cotton, PP and blended fabric of cotton (35%) and PET (65%)	PDA NPs	$^{1H,1H,2H,2H}$ - perfluorodecanethiol	2.0	T-HCl	2	—	AgNO <sub>3</sub>	—	—
Pristine fabric	PDA NPs	PDMS	80 mg/40 mL	Alkaline	24	R. T.	SiO <sub>2</sub>	—	95
Other materials	PDA NPs	OTESO	0.4 g	T-HCl	10	R. T.	SiO <sub>2</sub>	—	—
Cotton	PDA NPs	<i>n</i> -DDT	2.0	25% NH <sub>4</sub> OH	24	60	AgNO <sub>3</sub> , CuSO <sub>4</sub> (hexane) <sup>e</sup>	72 172.9 ( <i>n</i> ->99 14 460.3 (diesel))	—
Cotton	PDA NPs	DDT	2.0	T-HCl	24	R. T.	FeCl <sub>3</sub> ·6H <sub>2</sub> O	—	>98
Cotton	PDA NPs	SA	2.0	T	4	25	CuSO <sub>4</sub> ·5H <sub>2</sub> O	—	—
Polyvinylidene fluoride (PVDF)	PDA NPs	HS(CH <sub>2</sub> ) <sub>11</sub> CH <sub>3</sub> / HS(CH <sub>2</sub> ) <sub>10</sub> COOH (Thiol)	2.0	T-HCl	24	40	AgNO <sub>3</sub>	11 000 (light oil/water mixture)	99.2% (light oil/water mixture)
								96.5% (heavy oil/water mixture)	*Rapid stimulus responsibility, superior wettability switching ability, comparable permeability and high separation efficiency



Type of fabric/ textile	Modification materials		Optimum coating parameters				Highest oil permeation flux (L m <sup>-2</sup> h <sup>-1</sup> )	Separation efficiency (%)	Durability features	Ref.
	Surface roughness	Surface energy	DA conc. (mg mL <sup>-1</sup> )	Buffer mL	Time (h)	Temp. (°C)	Other materials			
Cotton	PDA NPs	PDMS	100 mg/50 mL	T	60	12	CuSO <sub>4</sub> ·5H <sub>2</sub> O, ZIF-8 nanomaterials	—	—	87
Cotton	PDA NPs	Hexa decyl tri methoxy silane	2	T-HCl	12 hours stirring/24 freeze drying	R. T.	FeCl <sub>3</sub> ·6H <sub>2</sub> O	8561.02	99.5	*Energy-saving separation of multiphase oil/water mixtures and emulsions
Woolen felt	PDA NPs	DDT	0.01	T-HCl	14	R. T.	AgNO <sub>3</sub> , TiO <sub>2</sub>	—	—	88
PP fibre	PDA NPs	3-Aminopropyltriethoxysilane (APTES)	200 mg L <sup>-1</sup>	T-HCl	12 h reaction/ 5 h immersion	R. T.	MXene nanosheets, polyppyrrole (PPY), pH responsive polymer (PDM)	—	—	*Excellent photocatalytic properties
Cotton	PDA NPs	PDMS	2	—	12	R. T.	MWCNT	16.21 m <sup>3</sup> m <sup>-2</sup> h <sup>-1</sup>	99	*Low cost, bio-degradable and self-extinguishing properties
Nylon 56	PDA NPs	Trimethylaminomethane, tetraallyl silane	400 mg/200 mL	—	0.5	60	3-Mercaptopropionic acid, methyl siloxane- dimethyl siloxane copolymer (mercapto)	>98	>98	90
										91
										92
										93
										94

<sup>a</sup> Abbreviations: T = Tris-buffer; P = phosphate buffer; R. T. = room temperature; PDA NPs = polydopamine nanoparticles; SDA = structure directing agent; SiO<sub>2</sub> = silicon dioxide; NH<sub>4</sub>OH = ammonium hydroxide; CuSO<sub>4</sub> = copper sulphate; AgNO<sub>3</sub> = silver nitrate; FeCl<sub>3</sub>·6H<sub>2</sub>O = ferric chloride.



Table 2 PDA-coated superhydrophilic/underwater superoleophobic textiles for oil/water separation

Type of fabric/textile	Surface roughness	Optimum coating parameters				Other materials	Water permeation flux ( $\text{L m}^{-2} \text{h}^{-1}$ )	Pressure (MPa)	Durability features	Separation efficiency (%) (recyclability)	Ref.
		DA conc. (mg mL <sup>-1</sup> )	Buffer	Time (h)	Temp. (°C)						
Cotton	PDA NPs	4.0	T-HCl	24	R. T.	Chitosan	15 100–30 000	—	>99	*Outstanding chemical and mechanical resistance	93
Polyester fabric	PDA NPs and PEI	2.0	T	7	—	Sodium periodate ( $\text{NaIO}_4$ ), hydrogen peroxide ( $\text{H}_2\text{O}_2$ ) and copper sulfate ( $\text{CuSO}_4$ )	>115 000	Gravity	>99.2	*Resistance to extreme environments and long term durability	94
Cotton	PDA NPs and $\text{TiO}_2$	120	T-HCl	—	—	(3-Aminopropyl) triethoxysilane (KH550, 99%), copper sulfate pentahydrate ( $\text{CuSO}_4 \cdot 5\text{H}_2\text{O}$ ), polyethylene glycol (PEG)	32 000	Gravity	99.9	*Resistance to salt solution, acids and abrasion	95
Polyarylene ether nitrile (PEN) nanofibrous mat	PDA NPs	—	T-HCl	4	R. T.	Hexagonal boron nitride (h-BN), $\text{CuSO}_4$ , $\text{H}_2\text{O}_2$	588.1 (emulsion) 8400 (oil/water mixture)	0.04	>99	*Resistance to harsh environments and antifouling ability	96
Thermoplastic polyurethane	PDA NPs	—	T	—	—	Multi-walled carbon nanotubes	4195–7240	0.05	99.9	*Enhanced mechanical properties, thermal stability and electrical conductivity	97
Poly acrylonitrile fibre (PAN)	PDA nano spheres	40 mg	T-HCl	7	25	—	1570 $\text{L m}^{-2} \text{h}^{-1} \text{bar}^{-1}$	—	96.1	*Excellent anti-oil adhesion properties	98
Pristine material	PDA nano spheres	0.5 g/10 mL	—	48	R. T.	$\text{AgNO}_3$	—	—	99.3	*Good separation efficiency and durability	98
Polyvinylidene fluoride (PVDF)	PDA NPs	2.0	T-HCl	24	40	$\text{AgNO}_3$ and thiols	2500	Gravity	>99	*Outstanding cycle performance and antibacterial activity	99
Micro cellulose ester membrane (MCEM)	PDA NPs	0.2g/100 mL	T-HCl	12	R. T.	HAP, $\text{SiO}_2$ , Tetraethoxysilane(TEOS)	2000–7000	—	90.90	*Superwettability and superior pH responsibility *Improved tensile strength and mechanical stability *Resistance to acidic/alkaline/salt solutions	100



Table 2 (Contd.)

Type of fabric/textile	Surface roughness	Optimum coating parameters					Water permeation flux (L m <sup>-2</sup> h <sup>-1</sup> )	Pressure (MPa)	Separation efficiency (%) (recyclability)	Durability features	Ref.
		DA conc. (mg mL <sup>-1</sup> )	Buffer	Time (h)	Temp. (°C)	Other materials					
Bacterial cellulose (BC)	PDA NPs	0.46 g/150 mL	T	24	R. T.	TiO <sub>2</sub> , sodium alginate	7428–8774 (heavy oil) 9597–10 000 (light oil)	—	>99	*Low cost, non-toxic and eco friendly	101
Cotton	PDA NPs	5 mg mL <sup>-1</sup>	T-HCl	1 h sonication/ 4 h immersion/24	R. T.	Carbon nanotubes	10 834	Gravity	>99.8	*Excellent anti-pollution and photo catalytic properties	102
Cotton	PDA NPs	4	T-HCl	24	R. T.	SiO <sub>2</sub> , TEOS	8100–34 000 (various oils)	Gravity	>99	*Outstanding cationic dye adsorption capacity	103

\*Separation flux of light oil 3000 L (m<sup>2</sup>.h)<sup>-1</sup>  
\*Oil discharge rate of heavy oil can reach 98.95%  
\*Excellent stability and durability under harsh conditions  
\*Continuous separation of crude oil/water (15 times) and toluene/water (100 times)

membranes to separate oil/water mixtures by a filtration strategy that is beneficial for continuous and large-scale separations.<sup>41–43</sup>

The surface wettability of various textiles has been modified by using different strategies such as grafting, dip-coating, spray-coating, chemical vapor deposition, solution immersion, and *in situ* polymerization. The fabrication of superhydrophobic textiles has been achieved by using a wide range of materials/chemicals/techniques, which aim to: (1) increase the surface roughness,<sup>44</sup> and (2) reduce the surface free energy of the modified fabrics. The presence of strong adhesion between the deposited materials (*e.g.*, nanoparticles) and the surface of the modified textiles plays an important role in making durable superwetting textiles with superior mechanical abrasion resistance, good recyclability, and corrosion resistance.<sup>45,46</sup> Good adhesion can be promoted *via* strong inter/intramolecular ionic interactions, covalent bonds, or ionic/covalent crosslinks.<sup>47,48</sup>

Polydopamine coatings, invented by Lee and Messersmith in 2007, have been employed extensively for fabricating various durable superwetting substrates, including fabrics and textiles.<sup>49–54</sup> In general, the PDA coating is prepared by chemical oxidative polymerization in the absence (pH = 8.5) or presence (neutral/acidic conditions) of organic/inorganic oxidants.<sup>52–54</sup> The main requirement for chemical oxidative polymerization is the presence of an electron donor atom (*e.g.*, O, N, or S) with a high oxidation tendency to induce the initiation of the chain growth *via* the formation of cation/cation radical species.<sup>55</sup> Chemical oxidative polymerization has been employed for the fabrication of electrically conducting polymers such as polyaniline, polypyrrole and polythiophene.<sup>56–60</sup> The oxidative polymerization of polydopamine is depicted in Fig. 1A. The versatility of the polydopamine coating is due to its ease of application as well as its ability to adhere to various surfaces (metals, plastics, ceramics, *etc.*) by a simple solution immersion and *in situ* deposition process.<sup>61–63</sup> Depending on the modification process, materials used and the chemical composition of the textile surface, the adhesion of polydopamine to the fabric surface can be achieved *via* different surface interaction mechanisms including metal coordination, Michael-type additions and/or Schiff-base formations, hydrogen bonding, and  $\pi$ – $\pi$  stacking,<sup>48,52,64–67</sup> as shown in Fig. 1B. This review highlights the most recent literature studies related to the fabrication of superwetting textiles modified with polydopamine coatings for oil/water separation applications. The first part of the review is related to SHB textiles, the second part is devoted to the SHL/UWSOB textiles, and the final section discusses the separation of emulsions. In addition, the recent related studies have been presented and summarized in Tables 1 and 2.

## 2. Review for the models of wettability

The effectiveness of separating oil/water mixtures highly depends on the membrane surface's wettability, which was determined by how easily the liquid could penetrate the solid surface. When the liquid droplet contacts a solid surface in the atmosphere, it creates a three-phase boundary where the solid,

liquid, and gas phases intersect.<sup>104</sup> Notably, the characteristics of the wetted surface are frequently described *via* the contact angle (CA) and the sliding angle (SA). The CA indicates the equilibrium of surface tension forces among the solid, vapor, and liquid interfaces, and the solid substrate behaves as a static surface. Conversely, the SA is utilized to gauge the dynamic behavior of a solid surface concerning wetting. Significantly, in the wetting process, the system achieves its lowest energy state when the droplet reaches the equilibrium.<sup>105</sup> Based on the value of the CA ( $\theta$ ), the wetting behavior is categorized into four primary types, as shown in Fig. 2. The surface is classified as hydrophilic if the CA falls in the range of 10°–90° (Fig. 2a). However, the superhydrophilic surfaces have a CA lower than 10°. They exhibit a strong affinity for water, resulting in the spontaneous spreading of water droplets and full surface wetting. As shown in Fig. 2b, hydrophobic surfaces exhibit contact angles in the 90°–150° range, allowing the liquid droplets to not spread uniformly within the surface. As a result, they reject water and exhibit a lower affinity for liquids. In comparison, superhydrophobic surfaces represent an extreme form of hydrophobicity. These surfaces have contact angles greater than 150°, causing water droplets to form almost perfect spheres and roll off the surface easily. Superhydrophobic surfaces are characterized by their outstanding water-repellent properties and self-cleaning capabilities.<sup>106,107</sup>

The wetting phenomena have been described using Young, Wenzel, and Cassie–Baxter models. Thomas Young introduced the concept of the CA for the solid/liquid interface. He discussed the cohesion of superficial particles at both solid and liquid surfaces. Additionally, once the tension at the interfaces reaches equilibrium, as illustrated in Fig. 2c, the correlation can be represented by Young's equation,<sup>26</sup> as indicated in eqn (1):

$$\cos \theta_Y = (\gamma_{SG} - \gamma_{SL})/\gamma_{LG} \quad (1)$$

In this context,  $\theta$  represents the equilibrium contact angle, while  $\gamma_{SG}$ ,  $\gamma_{SL}$ , and  $\gamma_{LG}$  represent the interfacial energies of the solid–gas, solid–liquid, and liquid–gas interfaces, respectively. Young's equation assumes an ideal scenario of a perfectly smooth, rigid, and homogeneous solid surface, which doesn't accurately reflect real-world surfaces that are often rough and heterogeneous. When water encounters a rough solid surface, it can exist in two states: (i) where water fully adheres to the solid surface, or (ii) where water adheres to the combined surface of solid and air, forming droplets known as fakir droplets.<sup>109</sup> Wenzel's model proposed that, due to varying degrees of rough microstructure on the solid surface, the liquid would completely occupy the surface microstructure upon contact with the solid. He incorporated a roughness coefficient ( $R$ ) into Young's equation, thereby creating the Wenzel model shown in eqn (2):

$$\cos \theta_W = R \cos \theta_Y \quad (2)$$

where  $\theta_W$  is the apparent rough surface's contact angle,  $\theta_Y$  is the plane's inherent Young contact angle, and  $R$  is the roughness factor, which represents the proportion of the actual surface area compared to the surface area of a rough solid substrate.



According to the above equation, the surface roughness has an impact on wettability, which can be enhanced or decreased by  $R$ . If a liquid droplet prefers to wet the surface, *i.e.*  $\cos \theta_Y > 0$ , the roughness factor ( $r$ ) will exceed one. In this context, the surface roughness amplifies the wetting behavior, resulting in an apparent contact angle ( $\theta_W$ ) that is larger than the equilibrium contact angle ( $\theta_Y$ ). This situation is referred to as the "Wenzel wetting regime". Conversely, if the liquid forms droplets on the surface, *i.e.*  $\cos \theta_Y < 0$ ,  $R$  will be  $<1$ . Surface roughness inhibits wetting behavior, leading to a lower apparent CA ( $\theta_W$ ) than the equilibrium CA ( $\theta_Y$ ). This phenomenon is known as the "Wenzel non-wetting regime" (Fig. 2d). The Wenzel model's principle focuses on understanding surface roughness's influence on

wetting behavior. Thereby, it enables the prediction of the apparent CA on rough surfaces by considering the properties of the smooth surface and the roughness factor.<sup>106,110</sup>

Increasing surface roughness and reducing feature size can cause a liquid droplet to be suspended above the rough surface structure, trapping small amounts of air beneath the liquid in pits or grooves. This phenomenon was explained by the Cassie–Baxter model according to the following eqn (3) and Fig. 2e:

$$\cos \theta_{CB} = f_{SL} \cos \theta_1 + f_{LG} \cos \theta_2 \quad (3)$$

where  $\theta_{CB}$ ,  $\theta_1$  and  $\theta_2$  are the apparent CA of the droplet on the rough surface, the solid surface, and the air pockets or gaps, respectively.  $f_{SL}$  and  $f_{LG}$  are the area fractions of the solid–liquid

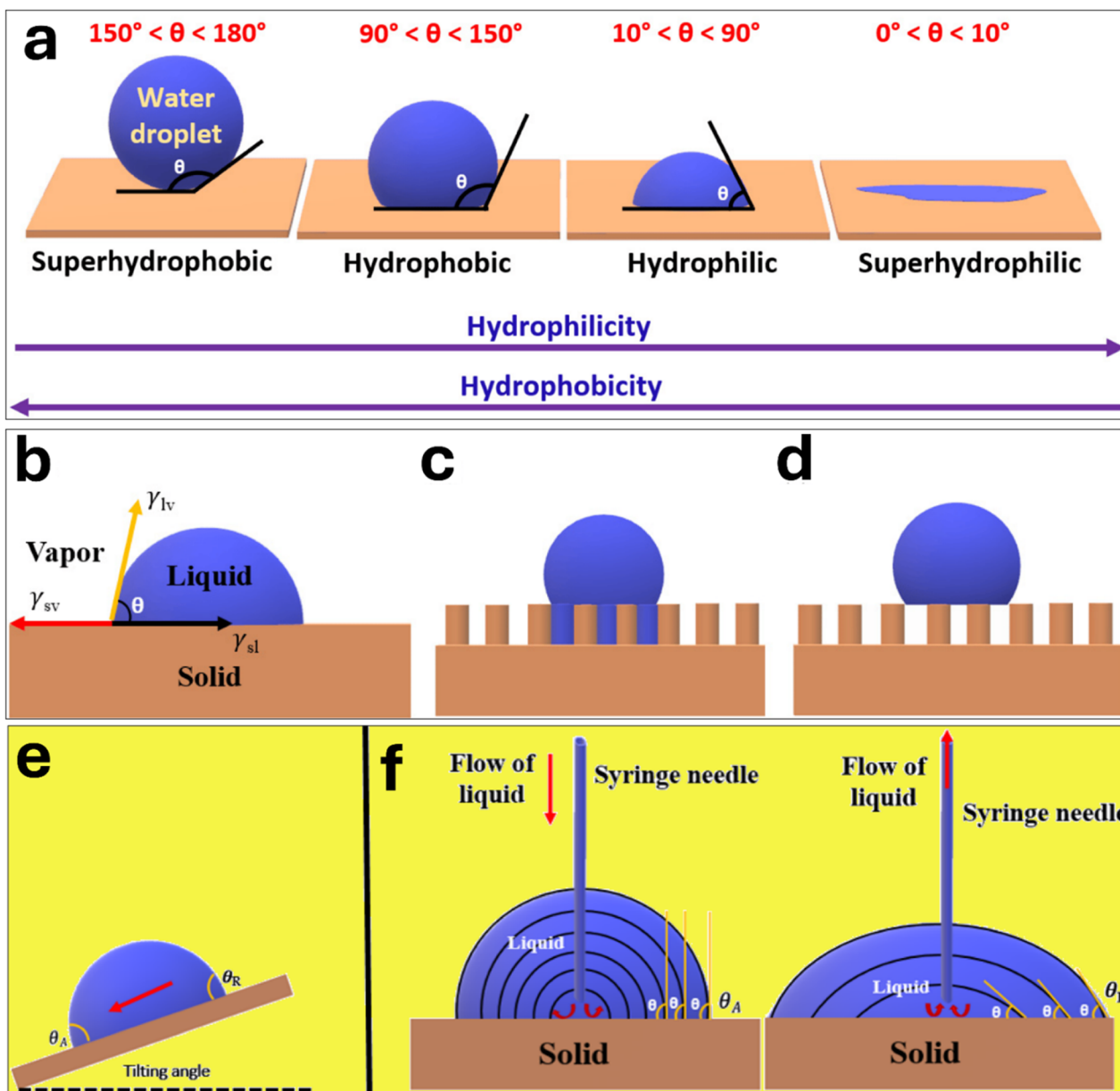


Fig. 2 Schematic illustration of various wettability states: (a) an illustration of wetting models based on Young's model (b), Wenzel's model (c), and Cassie–Baxter's model (d); measuring the advancing and receding angles by (e) tilting the substrate; and (f) changing the droplet volume by gradually introducing or extracting liquid from a sessile droplet, ref. 108.



phase and liquid–gas phase, respectively. The model considers the contributions of both the solid surface and the air pockets to the overall contact angle, leading to a higher apparent contact angle compared to the Wenzel model, which assumes the total wetting phenomenon of a rough surface.<sup>106,111</sup>

Contact angle hysteresis (CAH) refers to the difference between the advancing contact angle ( $\theta_a$ ) and the receding contact angle ( $\theta_r$ ) of the droplet.  $\theta_a$  is the angle generated as the droplet spreads on the surface, whereas  $\theta_r$  is created when the droplet retracts from the surface. Contact angle hysteresis exists because contact lines usually do not slide freely. Real surfaces are amorphous, deformable, rough, and show different crystalline orientations, leading to the observed contact angle hysteresis.

### 3. PDA-coated superhydrophobic (SHB) textiles for oil/water separation

#### 3.1. Cotton textiles

Wang *et al.* fabricated a PDA-coated superhydrophobic fabric, composed of a polyester (65%) and cotton (35%) blend, by using a two-step modification process,<sup>69</sup> as shown in Fig. 3A. The surface roughness was achieved by using folic acid (FA) as a structure directing agent (SDA) during the deposition of PDA NPs, while

octadecylamine (ODA) was employed as a low surface energy material which endowed the modified textiles with a superhydrophobic character as revealed from the high WCA (162°), and the low WSA (7°). The construction of a hierarchical rough morphology was achieved by the controlled addition of DA and FA, which was followed by the addition of the Tris–HCl buffer solution after a stirring period of 1 hour. As illustrated in Fig. 3A, self-driven, energy-saving, and highly efficient crude oil spill cleanup was achieved by using a mini boat made from the modified superhydrophobic textiles and floated on the top of crude oil-polluted water. This mini boat absorbed all the crude oil and accumulated inside the cavity for 10 min with a cleanup efficiency of 97.1%.

Liu *et al.* fabricated self-healing superhydrophobic cotton fabrics, coated with PDA microcapsules, by using a one-step modification process.<sup>70</sup> The pristine cotton fabric was dipped into an emulsion containing a low surface energy material (ODA or octadecanethiol ODT), Tris–HCl buffer, and DA (0.5 mg mL<sup>-1</sup>) for a total period of 12 hours. After plasma treatment, the modified superhydrophobic fabric lost its hydrophobicity and became hydrophilic, as shown in Fig. 3B and C. However, upon mechanical action on the fabric (compression/stretching), the self-healing property was demonstrated with a full recovery of its superhydrophobic nature. This self-healing property was

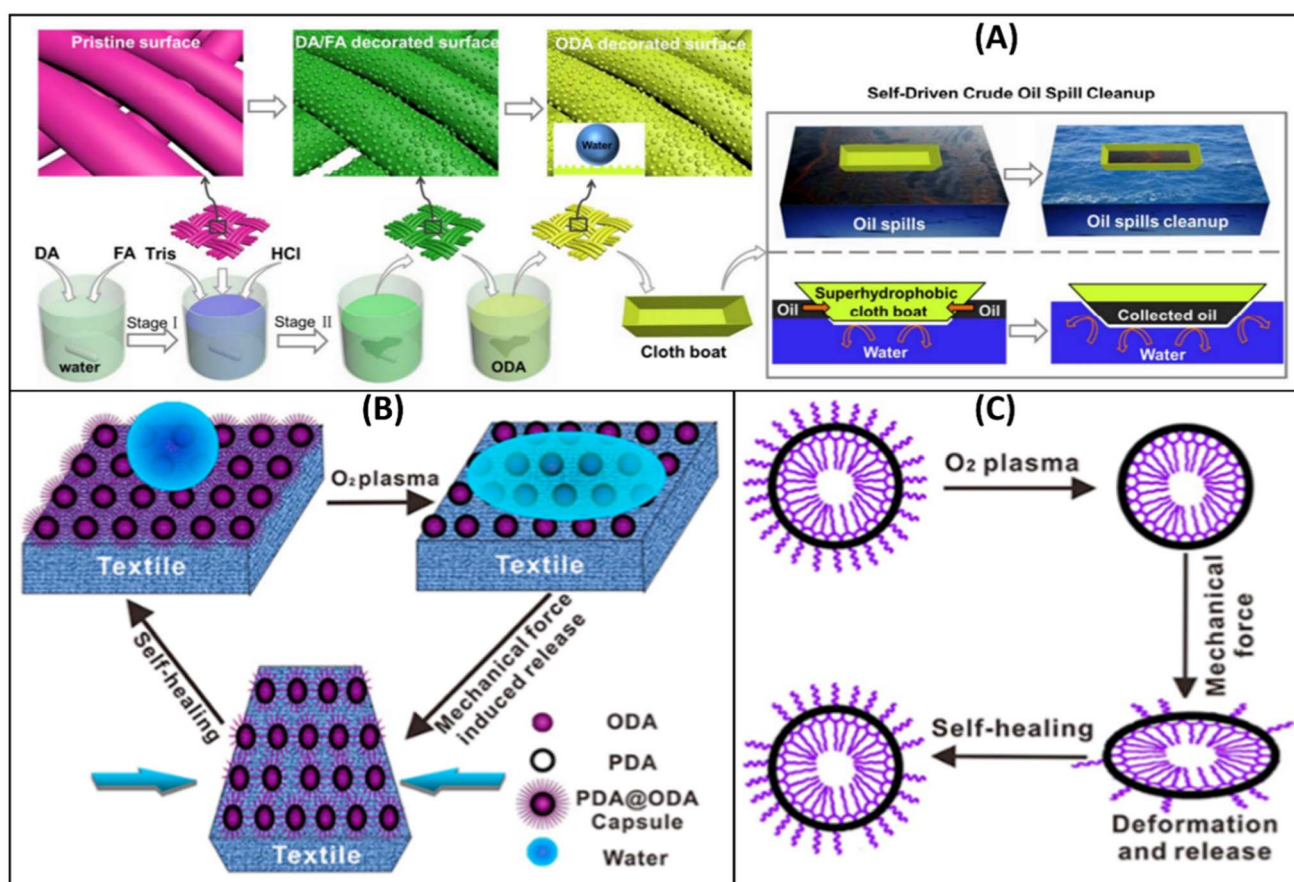


Fig. 3 Schematic illustration of the fabrication of a superhydrophobic fabric with a micro-nanostructure via a novel mussel-inspired approach, and a superhydrophobic cloth boat made from the fabric for self-driven oil spill cleanup (A), reproduced with permission from ref. 69. Regeneration of hydrophobicity through mechanical stimulation (B) and mechanism in the self-healing process during compression (C), reproduced with permission from ref. 70.



attributed to the release of the low surface energy materials (ODA or ODT) embedded in the coated PDA microcapsules (Fig. 3B and C).

Guo *et al.* reported a simple one-pot method to fabricate a robust superhydrophobic cotton fabric by the solution immersion method.<sup>72</sup> The surface roughness was achieved by

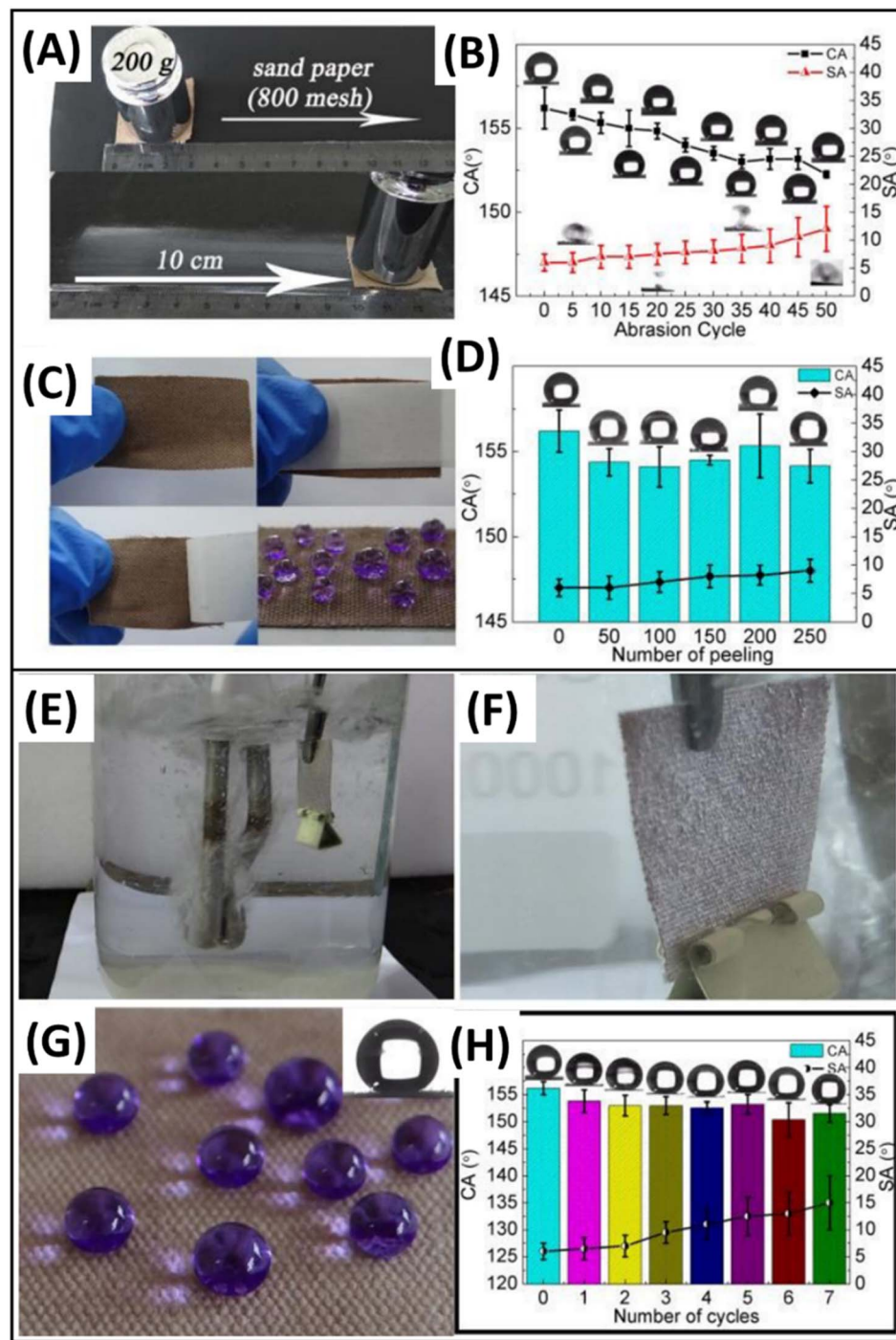
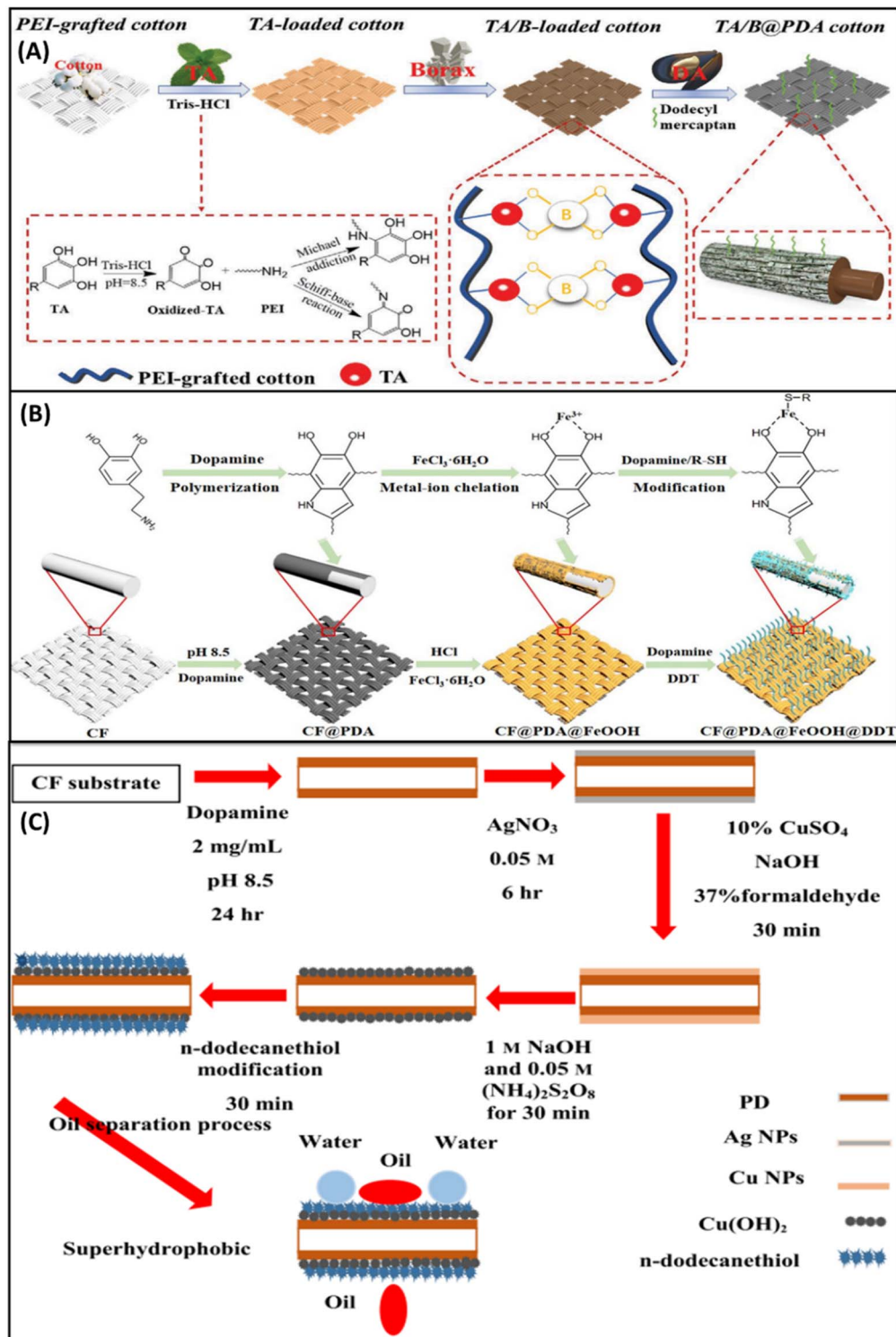


Fig. 4 (A) Photographs showing the abrasion process. (B) Contact angle and sliding angle of the superhydrophobic fabric after each abrasion cycle. The optical images of the static water droplets (5  $\mu$ L) after each abrasion cycle are shown in the insets. (C) Photographs showing the tear test process and water droplets (dyed with crystal violet) on the fabric surface after the test. (D) Contact angle and sliding angle of the superhydrophobic fabric after each tear test cycle. The optical images of the static water droplets (5  $\mu$ L) after each cycle are shown in the insets. (E) Photograph of the superhydrophobic PDA@SiO<sub>2</sub> coated cotton fabric immersed in boiling water. (F) A stable, silver mirror-like phenomenon of the fabric immersed in boiling water. (G) Photograph of water (dyed with crystal violet) standing on the fabric treated in boiling water for 5 min. Optical image of the static water droplets (5  $\mu$ L) after 5 min of boiling-water treatment is shown in the inset. (H) Water contact angle and sliding angle of the tested fabric after each 5 min boiling-water treatment. Optical images of the static water droplets (5  $\mu$ L) after each 5 min boiling-water treatment are shown in the insets, reproduced with permission from ref. 72.



the combined effect of PDA and silicon dioxide ( $\text{SiO}_2$ ) through the copolymerization process at room temperature and the lower surface energy was attained by the presence of methyl groups on the PDA/ $\text{SiO}_2$ -coated superhydrophobic fabric. The modified fabric exhibited a separation efficiency of 99.9% and

a permeation flux of  $\sim 4000 \text{ L m}^{-2} \text{ h}^{-1}$  with a stable performance even after 20 separation cycles. The modified fabric showed excellent mechanical durability for various tests (abrasion, peeling, and ultrasonic treatment), as shown in Fig. 4A-D. The functionalized fabrics showed high durability in harsh



**Fig. 5** Schematic illustration for the preparation of superhydrophobic cotton fabrics: (A) TA/borax coating, reproduced with permission from ref. 74; CF/PDA/FeOOH/DDT (B), reproduced with permission from ref. 79; CF with aligned Cu(OH)<sub>2</sub> nanoneedles (C), reproduced with permission from ref. 78.

chemical environments, UV irradiation, and boiling water (Fig. 4E–H).

Luo *et al.*, reported the fabrication of a flame retardant superhydrophobic polyethylene imine (PEI) grafted cotton fabric coated with the biologically derived materials of tannic acid (TA), borax, and PDA by a dip-coating method,<sup>74</sup> as shown in Fig. 5A. Borax was utilized to attain the flame-retardant property. However, when it comes into contact with water during washing, the borax will dissolve. Hence, TA was used to

make a complexation with borax with the additional benefit of oxygen-free radical scavenging and carbonization ability during combustion. The functionalized cotton fabric displayed a WCA of  $153.30 \pm 1.2^\circ$ , a WSA of  $9^\circ \pm 0.8^\circ$ , and an oil/water separation efficiency of >98% after 30 cycles. The residual content during thermal studies at  $800\text{ }^\circ\text{C}$  under nitrogen and oxygen atmospheres is about 48.9% and 27.9%, respectively, clearly showing the improved thermal stability of the modified fabric as depicted in Fig. 6A–D.

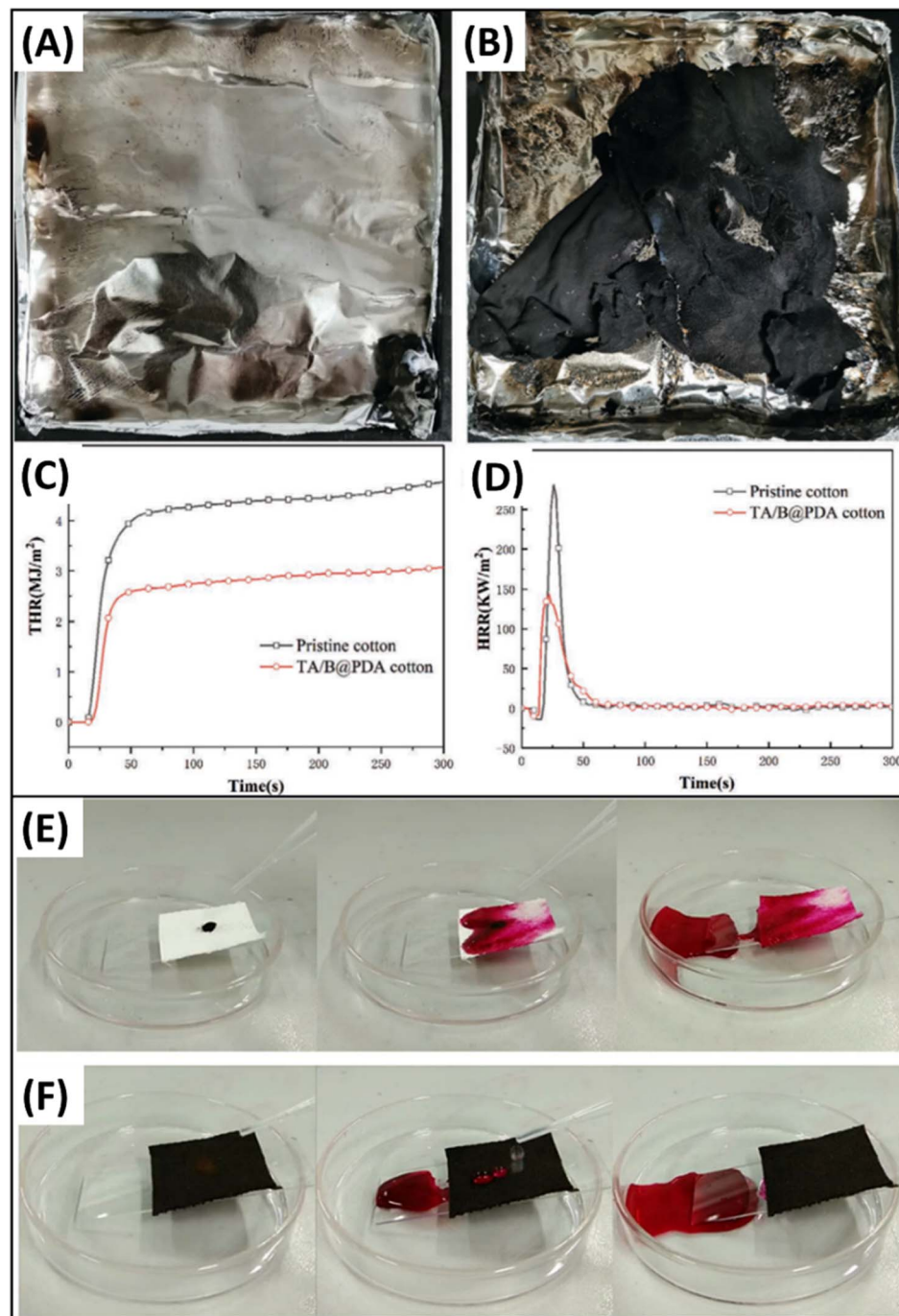


Fig. 6 Digital photographs of char residues of (A) pristine cotton and (B) TA/B@PDA cotton fabrics after CCT. (C) THR and (D) HRR of cotton samples, reproduced with permission from ref. 74; illustrations of fabric with reactive red dye powder under rinsing with water: (E) original cotton fabric and (F) Fe/PDA/ODA cotton fabric, reproduced with permission from ref. 5.



Cheng *et al.* deposited  $\beta$ -FeOOH nanorods on the PDA-coated cotton fabric by an *in situ* hydrothermal process to provide roughness on the surface<sup>84</sup> (Fig. 5B).

Superhydrophobicity (WCA  $\sim 151^\circ$ ) and lipophilicity (OCA  $\sim 0^\circ$ ) were achieved by the addition of 1-DDT on the PDA/ $\beta$ -FeOOH deposited cotton fabric to reduce the surface energy. The

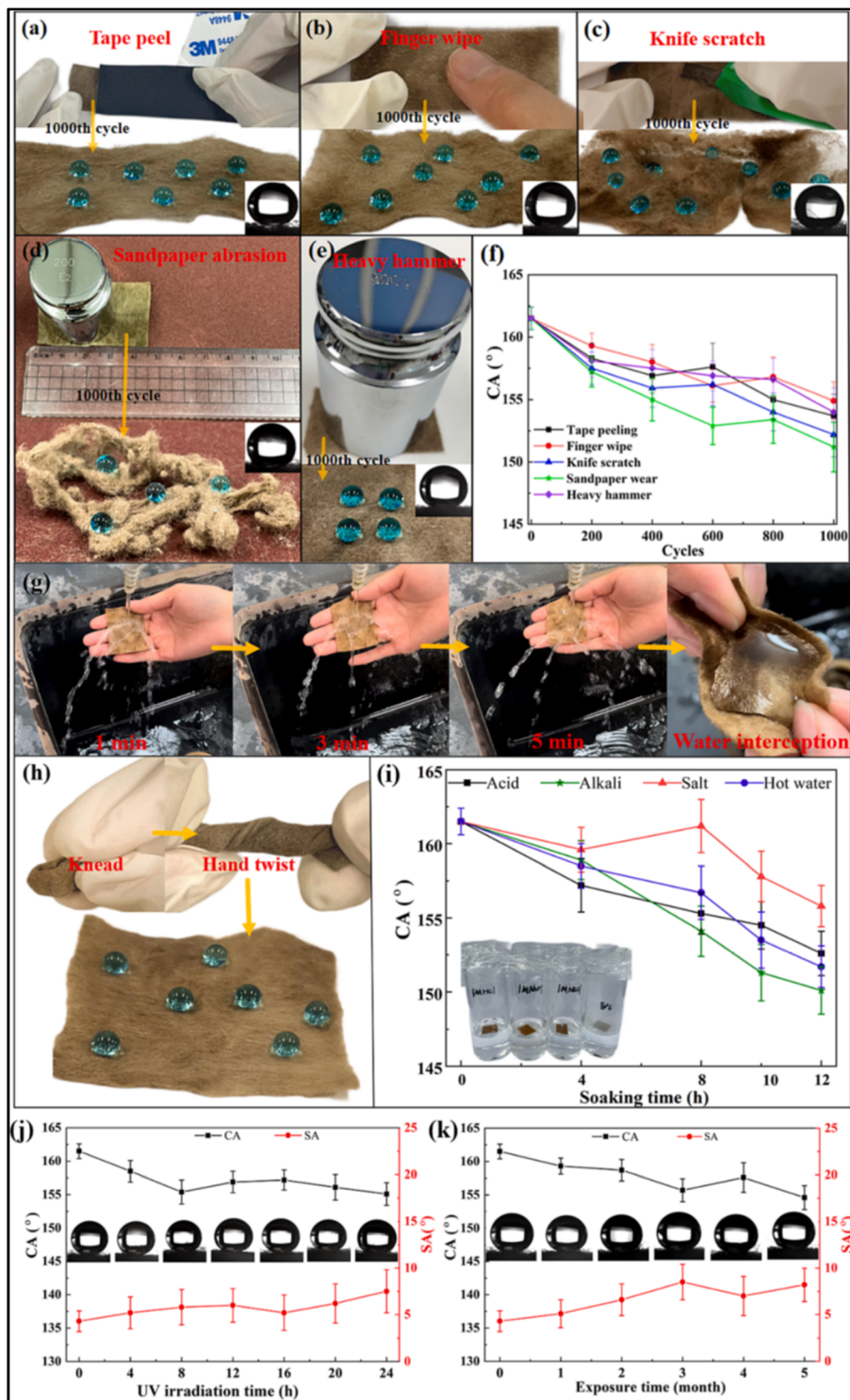


Fig. 7 Robustness of HFPC membranes. (a) Tape peel, (b) finger wipe, (c) knife scratch, (d) sandpaper abrasion, (e) heavy hammering, and superhydrophobic photographs of the corresponding 1000 cycles. (f) The corresponding changes in CAs after 1000 cycles. (g) Effective water interception even after 5 min of running water impact. (h) Elasticity test. (i) The superhydrophobic behavior after soaking in organic solvents (1 M  $\text{H}_2\text{SO}_4$ , 1 M NaOH, and 1 M NaCl) and 80 °C hot water for 12 h. Changes in CAs and SAs after (j) UV irradiation for 24 h and (k) outdoor weathering for 5 months. Reproduced with permission from ref. 88.



modified fabric exhibited higher oil–water separation efficiency for all types of oils, which is greater than 98% after 50 cycles. Enhanced thermal stability and excellent photocatalytic performance after 5 cycles were observed in the modified fabric due to the development of an even layer of  $\beta$ -FeOOH nanorods on the PDA-coated fabric.

Belal *et al.* synthesized copper hydroxide nanoneedles on the PDA-coated cotton fabric by the solution immersion process<sup>83</sup> (Fig. 5C). *In situ* polymerization of DA was carried out on the cotton fabric, followed by the addition of Ag nanoparticles (reduction) and Cu nanoparticles (oxidation), which endowed the surface with roughness. Thereafter, the low surface energy material of *n*-dodecanethiol (*n*-DDT) was coated on the functionalized fabric to achieve superhydrophobicity. The functionalized fabric exhibited a higher WCA of 168° together with a higher oil–water separation efficiency of above 99% after 100 cycles. The attained values of WCA > 166° after the solvent immersion (32 days) and exposure to acidic/basic conditions (48 hours) reveal water repellency and stability of the functionalized fabric.

Yan *et al.* reported a two-step procedure for fabricating the PDA-coated superhydrophobic cotton fabric grafted with ODA through a Schiff base reaction in the presence of  $\text{FeCl}_3$  by the solution immersion method.<sup>76</sup> The modified fabric showed excellent stability in harsh environments of varied pH, laundering, and organic solvents, with a WCA > 150° and WSA < 14°. However, it shows poor acid resistance due to the hydrolysis of amino groups in ODA and poor resistance to carbon tetrachloride ( $\text{CCl}_4$ ) as the ODA will be leached out in  $\text{CCl}_4$ . The functionalized fabric showed an oil/water separation efficiency of above 99% after 20 cycles. As illustrated in Fig. 6E and F, the functionalized fabric showed self-cleaning properties with good mechanical durability.

Chen and Guo fabricated the PDA-coated superhydrophobic fabric composed of a polyester (65%) and cotton (35%) blend by the solution immersion method.<sup>78</sup> The initial step involved forming a PDA coating *via* oxidation with sodium periodate, resulting in a modified textile characterized by hierarchical surface roughness. In the second step, superhydrophobicity was achieved by the incorporation of low surface energy ODT molecules. The functionalized fabric showed excellent superhydrophobic and self-cleaning properties with a WCA of 154° and a WSA of 9.5°. The modified fabric showed a separation efficiency of greater than 97% and a permeation flux of 4500 L m<sup>-2</sup> h<sup>-1</sup> even after 20 absorption/squeezing cycles.

Wang *et al.* employed a solution immersion method and thiol–ene click reaction to fabricate a superhydrophobic fabric composed of a blend of 50% cotton fiber and 50% nylon-56 fiber for oil–water separation with a self-cleaning ability.<sup>79</sup> The modified fabric was prepared by immersing the PDA-coated fabric into the mercaptopropylmethyl dimethoxy silane (MPMDS) under prescribed conditions. Thereafter, superhydrophobicity was achieved by treating the mercapto-modified fabric with a mixture of hexadecyl mercaptan, octavinyl-POSS, and 2,2-dimethoxy-2-phenylacetophenone (DMPA) to provide low surface energy along with the micro–nano rough surface. The modified fabric showed WCA and WSA of 162° and 8°,

respectively, with an excellent oil–water separation capacity. The durability of the modified fabric was evaluated by exposing the sample to mechanical abrasion, UV irradiation for 16 hours, immersion in an organic solvent for 24 hours, immersion in varying pH solutions (1 to 13) for 48 hours, and a laundering test for 4.5 hours. The results from the formed tests showed that the modified fabric did not lose its hydrophobicity with the WCA > 150° and WSA < 15°, which revealed the durability of the superhydrophobic fabric.

Xu *et al.* fabricated different PDA-coated superhydrophobic fabrics by using oxygen-induced polymerization of DA and the solution immersion method.<sup>80</sup> Deposition of PDA and silver nanoparticles provided the surface roughness, and further superhydrophobicity was achieved by the incorporation of 1*H*,1*H*,2*H*,2*H*-perfluorodecanethiol to attain the rough hierarchical structure and low surface energy. The modified fabrics showed WCA > 150° and WSA < 10° with excellent oil–water separation and self-cleaning ability.

Dong *et al.* fabricated the eco-friendly, solar-induced self-healing superhydrophobic cotton fabric by the solution immersion and dip-coating methods.<sup>85</sup> An activator ( $\text{CuSO}_4/\text{H}_2\text{O}_2$ ) was used to deposit PDA onto the cotton fabric to attain a stable and uniform rough surface. Stearic acid (SA) with a concentration of 0.1 wt% was employed to reduce the surface energy due to its long alkyl chain. The modified fabric exhibited a WCA of 162° and a WSA of 7.8° with an oil–water separation efficiency of ~100% after 5 cycles. Durability and stability of the modified fabric were evaluated by an abrasion test for 1000 cycles, a laundering test for 5 cycles, and immersion in acidic/basic/alkaline solution for 24 hours, showing that the modified fabric did not lose its superhydrophobicity with the WCA > 150°. Furthermore, UV transmittance is <1% for the modified fabric and recovers its superhydrophobicity after 6 cycles of plasma treatment and light irradiation. The above results reveal the UV protection and self-healing properties of the modified fabric.

Zhu *et al.*, prepared the antibacterial composite cotton fabric by the dip-coating method.<sup>87</sup> Surface roughness was created by self-polymerized PDA NPs, and the antimicrobial effect was attained by the *in situ* growth of ZIF-8 nanomaterials, which act as a photo thermal agent, followed by incorporating PDMS to reduce the surface energy through the dip-coating process on cotton fabrics. The prepared composite fabric shows a WCA of 153° at 1 wt% PDMS, which shows the successful attainment of super wettable characteristics. Durability was assessed through 5 washing cycles and a friction distance of 100 cm, which exhibits the WCA > 140°. Additionally, ZIF-8 nanomaterials on the prepared fabric release positively charged  $\text{Zn}^{2+}$  under near-infrared light irradiation to rupture the bacterial cells, which enhances the antibacterial effectiveness.

Long *et al.*<sup>88</sup> fabricated the multifunctional super hydrophobic membrane with a significant photocatalytic effect on the cotton fabric through the impregnation and water bath heating method. They employed  $\beta$ -FeOOH NPs to achieve the photocatalytic characteristics and rough structure on the PDA coated cotton material. Furthermore, surface energy was reduced by the incorporation of hexadecyltrimethoxysilane at 60 °C for 5



hours to attain the hexadecyltrimethoxysilane/FeOOH/polydopamine/cotton fabric (HFPC) membrane. The as-prepared HFPC membrane guards the permeation of various liquids of muddy water, tea, urine, Coca-Cola and milk with a WCA of 153–158° and a SA of 6–7°, and rejects the various organic solvents which clearly reveals the successful attainment of superhydrophobicity and antifouling properties. As shown in Fig. 7, the outstanding chemical durability and mechanical robustness were assessed through various methods such as tape peeling (1000 times), finger wiping (60 kPa/1000 times), knife scratches (1000 times), abrasion test (1000 wears), hammering test (500 g/1000 times), water impact test ( $2.5 \text{ m s}^{-1}$  for 5 min),

kneading, hand twisting, stretching, chemical immersion (24 hours), UV aging (12 hours) and outdoor weathering test (5 months). Moreover, it has an efficient catalytic activity under visible light irradiation and a catalytic degradation ability of 99.5% under UV light irradiation through the photo-Fenton reaction. Additionally, it can separate oil–water mixtures continuously with an efficiency of up to 99.5%.

Zhang and Guo,<sup>91</sup> developed the self-healing durable cotton fabric for oil–water separation by a two-step process. They incorporated ZIF-8 on the cotton fabric along with PDA, as the combination of ZIF-8/dopamine (DA) can achieve quick assembly within 30 minutes on different material surfaces at

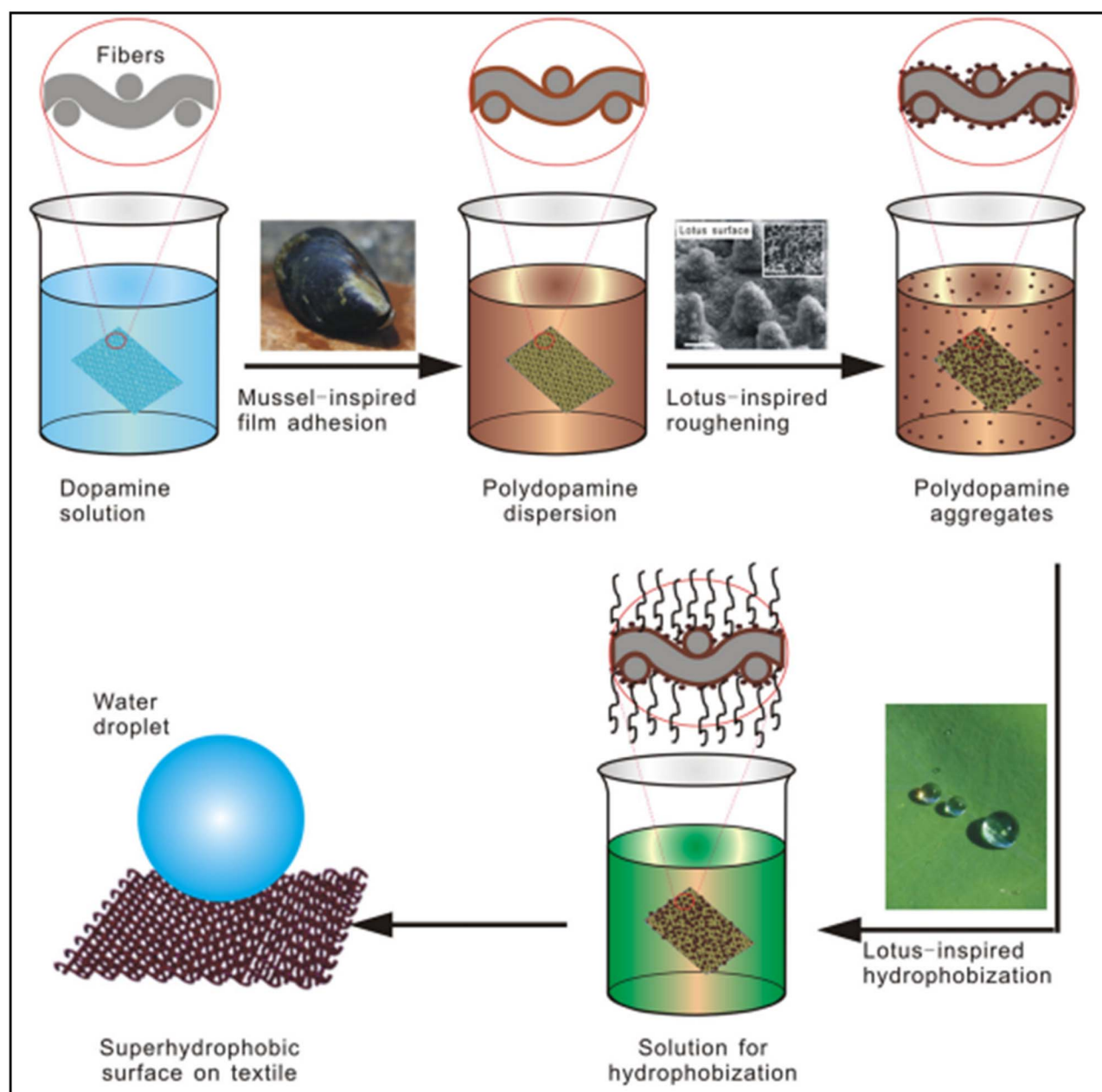


Fig. 8 Schematic illustration for the preparation of biomimetic superhydrophobic surfaces by combining mussel-inspired adhesion and lotus-inspired coating. Reproduced with permission from ref. 68.



neutral pH, which can enhance the self-healing properties. Besides this, multiwalled carbon nanotubes were added along with ZIF-8/DA through a solution immersion process on the cotton to attain mechanical stability.

The as-prepared fabric shows the separation efficiency of 99% with a WCA of  $158.9 \pm 1.4^\circ$  and a SA of  $4 \pm 0.5^\circ$ . In addition, it exhibits excellent resistance towards acidic solution (12 h), alkaline solution (6 h), ultrasonication (14 h) and abrasion (35 cycles) as the WCA is greater than  $145^\circ$  after the above-mentioned test. The as-prepared fabric surface retains its superhydrophobicity until 6 healing cycles, as revealed by the oxygen-plasma test due to the deposition of PDMS on the structural pores, which migrate rapidly to the surface driven by heat. However, self-healing of the microstructure on the modified fabric was not possible, as it would be demolished after abrasion, as detected by XPS.

### 3.2. Other SHB textiles

During the last few decades, researchers have focused on simple, eco-friendly, and sustainable methods to fabricate superhydrophobic materials. Eventually, mussels have drawn attention due to their uniqueness of discharging an adhesive protein to bind with all types of substrates.<sup>112</sup> PDA has been employed among researchers to mimic the mussel adhesion effect as it can be easily deposited on various substrates to achieve surface roughness. Additionally, it has properties of biocompatibility, oxidation resistance, and stability in near-infrared UV and visible light, as well as a high conversion efficiency for photothermal activity.<sup>113</sup>

Xue *et al.* fabricated a superhydrophobic PET fabric by using a two-step fabrication process,<sup>68</sup> as shown in Fig. 8. The surface roughness was attained *via* COP of DA in Tris buffer, which resulted in the deposition of PDA in the form of nanostructured papillae, while the superhydrophobicity was achieved in the subsequent step by immersing the modified textiles in 1% ethanolic solution of perfluorodecyl trichlorosilane (PFDTs). In an approach to mimic the lotus leaf nanostructured morphology, PET textiles were coated initially with DA in a phosphate buffer (pH = 8.5), followed by a second coating of DA in a Tris buffer. The former approach led to an increase in the WCA from  $150^\circ$  to  $160^\circ$  due to the hierarchical nanostructured morphology of the coated textiles caused by the production of larger PDA nanoparticles during the COP in phosphate buffer solution. The modified PET textiles exhibited properties including UV-shielding, good mechanical durability, and chemical stability in acidic and alkaline environments.

Lu *et al.* employed the polymer fiber fabric (tetra-copolyester and polypropylene) as a substrate to fabricate hierarchical rough structures to achieve superhydrophobicity by the simple bottom-up approach,<sup>75</sup> as shown in Fig. 9A. The fiber fabric was modified through dip coating by the incorporation of  $\text{SiO}_2$  NPs (obtained by the hydrolysis of TEOS) into the DA solution, with the successive immersion of the coated fabric into the silver ammonia solution containing 0.25 wt% of PVP (stabilizing agent). The incorporation of  $\text{SiO}_2$ , Ag NPs, and 1H,1H,2H,2H-perfluorodecanethiol (PFDT) endowed the fiber fabric with

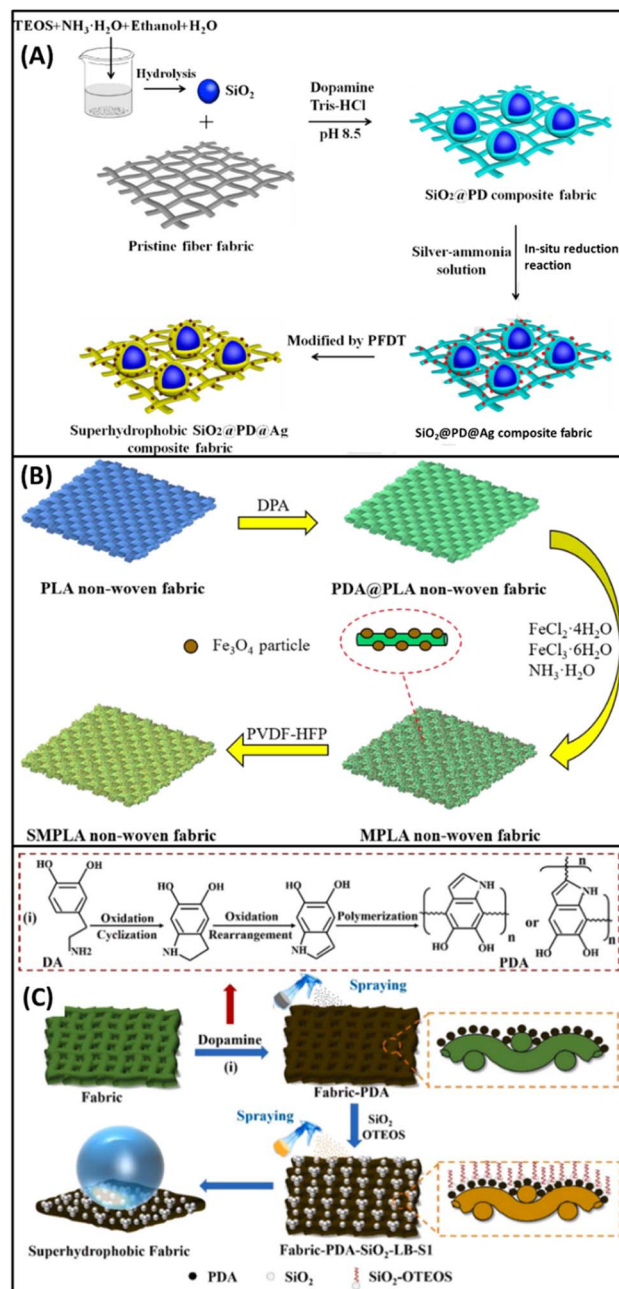


Fig. 9 Schematic illustration for the preparation of superhydrophobic fabrics (other than cotton): (A) tetra-copolyester and polypropylene/ $\text{SiO}_2$ /PD/Ag/PFDT, reproduced with permission from ref. 75; PLA/PDA/PVDF-HFP (B), reproduced with permission from ref. 77; other materials/PDA/ $\text{SiO}_2$ /OTEOS (C), reproduced with permission from ref. 82.

a micro/nano hierarchical rough structure and low surface energy. The exhibited separation efficiency of above 90% after 20 cycles shows the excellent stability and recyclability of the modified fiber fabric. However, after each cycle, there is a slight change in the WCA and WSA, which further sustains its water-repellency property. Additionally, the evaluated WCA of the modified fabric with the varied particle sizes of  $\text{SiO}_2$  (200, 300, and 400 nm) are  $147.8^\circ \pm 2.5^\circ$ ,  $154.5^\circ \pm 2.2^\circ$  and  $160.1^\circ \pm 2.8^\circ$ , respectively. Thus, the higher value of WCA shows the



superhydrophobicity of the modified fabric, and it can be increased by increasing the size of  $\text{SiO}_2$ .

Zeng *et al.* reported the fabrication of a bio-degradable superhydrophobic and magnetic poly(lactic acid) (PLA) nonwoven fabric for oil–water separation by the solution immersion method<sup>77</sup> (Fig. 9B). PDA was deposited on the PLA nonwoven fabric by an *in situ* polymerization of DA. Then the surface roughness and magnetic properties were achieved by the incorporation of ferrous chloride tetrahydrate ( $\text{FeCl}_2 \cdot 4\text{H}_2\text{O}$ ) and ferric chloride hexahydrate ( $\text{FeCl}_3 \cdot 6\text{H}_2\text{O}$ ) in the molar ratio of 1:2 to generate  $\text{Fe}_3\text{O}_4$  particles on the PDA coated PLA nonwoven fabric. Surface roughness and WCA can be increased by increasing the concentration of  $\text{FeCl}_3 \cdot 6\text{H}_2\text{O}$  (150 mmol L<sup>-1</sup>). Furthermore, the surface energy was reduced to attain superhydrophobicity by immersing the modified fabric ( $\text{Fe}_3\text{O}_4/\text{PDA}/\text{PLA}$ ) into the solution of poly(vinylidene fluoride-*co*-hexafluoropro-pylene) (PVDF-HFP) for 4 hours and drying at 50 °C for 1 hour. The modified nonwoven fabric displayed a WCA of 151.7°, which reveals the accomplishment of superhydrophobicity. Surface stability was evaluated by exposing the modified nonwoven fabric to different organic solvents, aqueous  $\text{H}_2\text{SO}_4$ , aqueous KOH solution, and boiling water for 96 hours. The measured WCAs are very close to the initial value, which reveals that the surface stability of the modified fabric is resistant to acid, alkali, and boiling water. Moreover, the attained WCA of 148.6° even after 20 cycles of the abrasion test further confirms the stability of the surface. The separation efficiency of the modified fabric shows more than 97% even after 20 cycles, exhibiting excellent recyclability. The absorption capacity shows that the modified nonwoven fabric can absorb organic solvent up to 16 times its weight, and it reaches 36 times in the case of higher density solvent  $\text{CCl}_4$ .

Zhang *et al.* reported the fabrication of a PDA-coated pristine superhydrophobic fabric by the combination of DA polymerization and the sol–gel method.<sup>81</sup> Surface roughness was achieved by the incorporation of PDA and  $\text{SiO}_2$  nanoparticles, and further superhydrophobicity was achieved by the involvement of polydimethylsiloxane (PDMS) to reduce the surface energy. The functionalized fabric showed an enhancement in its thermal stability and excellent oil–water separation efficiency of about 95% after 8 cycles, along with a WCA of 155°. Additionally, the functionalized fabric retains its superhydrophobicity with the WCA ~ 150°, after immersion in different pH solutions (1 to 13) for 24 hours, organic solvent for 24 hours, washing test for 3 hours, and exposure to UV irradiation for 1 hour.

Yu *et al.* employed various materials such as cotton fabric, sponge, concrete, wood, paper, glass, and aluminum sheet to fabricate superhydrophobic materials by the scalable two-step spraying method<sup>82</sup> as shown in Fig. 9C. PDA nanoparticles were utilized to attain the surface roughness and  $\text{SiO}_2$ /octyl-triethoxysilane (OTEOS) was incorporated to reduce the surface energy for the betterment of superhydrophobic properties. All the modified materials exhibited a WCA of  $154.2 \pm 2^\circ$  and a WSA of  $<3^\circ$ . The results attained from the durability and stability test reveal that the modified material has excellent resistance under mechanical abrasion, acidic/basic conditions for 24 hours, organic solvents immersion for 24 hours, UV

irradiation for 120 hours, and prolonged outdoor exposure for 12 months without losing its superhydrophobicity (WCA > 151°).

Su *et al.*<sup>86</sup> developed the pH responsive nanofibrous polyvinylidene fluoride (PVDF) membrane by the electrospinning process and further modification through solution immersion and a metal thiol co-ordination reaction. Surface roughness was attained by the incorporation of silver nanoparticles and successive addition of thiols ( $\text{HS}(\text{CH}_2)_{11}\text{CH}_3/\text{HS}(\text{CH}_2)_{10}\text{COOH}$ ), which further modifies the membrane into a pH responsive superwettable membrane. Self-polymerized DA restricts the mobility of silver nanoparticles and thiols, which creates the microstructure with upright structural stability against harsh mechanical action. The modified membrane showed the efficiency of over 99.2% for light oil/water and 96.5% for heavy oil/water mixtures. Mechanism of the wettability switching of the pH-responsive membrane is shown in Fig. 10A, which displays a WCA of 151.5° and UWOCa of 0° for pH = 7 and a WCA of 0° and a UWOCa of 152.5° (pH = 13). In addition, it exhibited the energy saving separation efficiency of about 99% for all types of surfactant stabilized emulsions with excellent durability and reusability.

Hatami *et al.*<sup>89</sup> utilized the waste woolen felt due to the benefits of fire retardant and self-extinguishing properties to prepare an oil–water separation material which is inexpensive and bio-degradable on top of that. They employed varied densities (1.165, 1.650, 1.682 and 1.747 g cm<sup>-3</sup>) of woolen felt as a base matrix, which is covered with  $\text{TiO}_2/\text{PDA}$  nanoparticles followed by silver nanoparticles through a solution immersion and stirring method to attain the rough hierarchical structure on the surface. Furthermore, the surfaces were modified with DDT to reduce the surface energy of the material and prepare the superhydrophobic/superoleophilic material. Among the modified superhydrophobic materials, the woolen felt material with a density of 1.650 g cm<sup>-3</sup> shows a WCA of 155.14° with a superior separation and passage of water at times of 4:19:120 and 1:37:100 (Fig. 10B), which is attributed to the homogeneous distribution of nanoparticles on the woolen felt which prevents the clusters.

Li *et al.*<sup>90</sup> constructed the pH responsive superhydrophobic composite membrane based on PP fibre, and the wettability was enhanced through PDA deposition on the substrate through *in situ* polymerization, solution immersion and vacuum assisted filtration methods. They used Mxene nanosheets, which are a 2D transition metal, due to the attributes of rich active sites, photo thermal properties, ceramic-like stability and polymer-like flexibility. Furthermore, to improve the stability and utilize photo thermal properties (Fig. 10C) of Mxenes, poly-pyrrole (PPy) was deposited on Mxenes through an *in situ* polymerization process. The vacuum assisted filtration method was used to construct the composite membrane, and its outer surface was covered with the transparent pH-responsive polymer PDM through a solution immersion process. The prepared composite membrane (PP-Mxene/PPy-PDM) at pH = 2 exhibits a WCA of 40° and an OCA of 130°. When the pH is elevated to 12, the WCA was 130°, and the OCA was 0°. The above results indicate that the membrane is hydrophilic in an acidic



environment and becomes hydrophobic in an alkaline environment. Moreover, it shows the higher separation efficiency ranging from 2.44 to 3.87 kg m<sup>-2</sup> h<sup>-1</sup> for the diverse oil–water emulsion with excellent resistance to abrasion, acidic and alkaline conditions.

Wang *et al.*<sup>92</sup> designated the Nylon 56 fabric to fabricate a superhydrophobic membrane through an eco-friendly

method because of its high elasticity, high temperature resistance, wear resistance and environmental protection. They coated this fabric with PDA, which can provide reactive sites for other ingredients, followed by the integration of tetraallyl silane (TETRA) and (mercapto) methyl siloxane-dimethyl siloxane copolymer (MMSDC) on the polydopamine coating by the thiol–ene click reaction under ultraviolet light. The hydrophobic

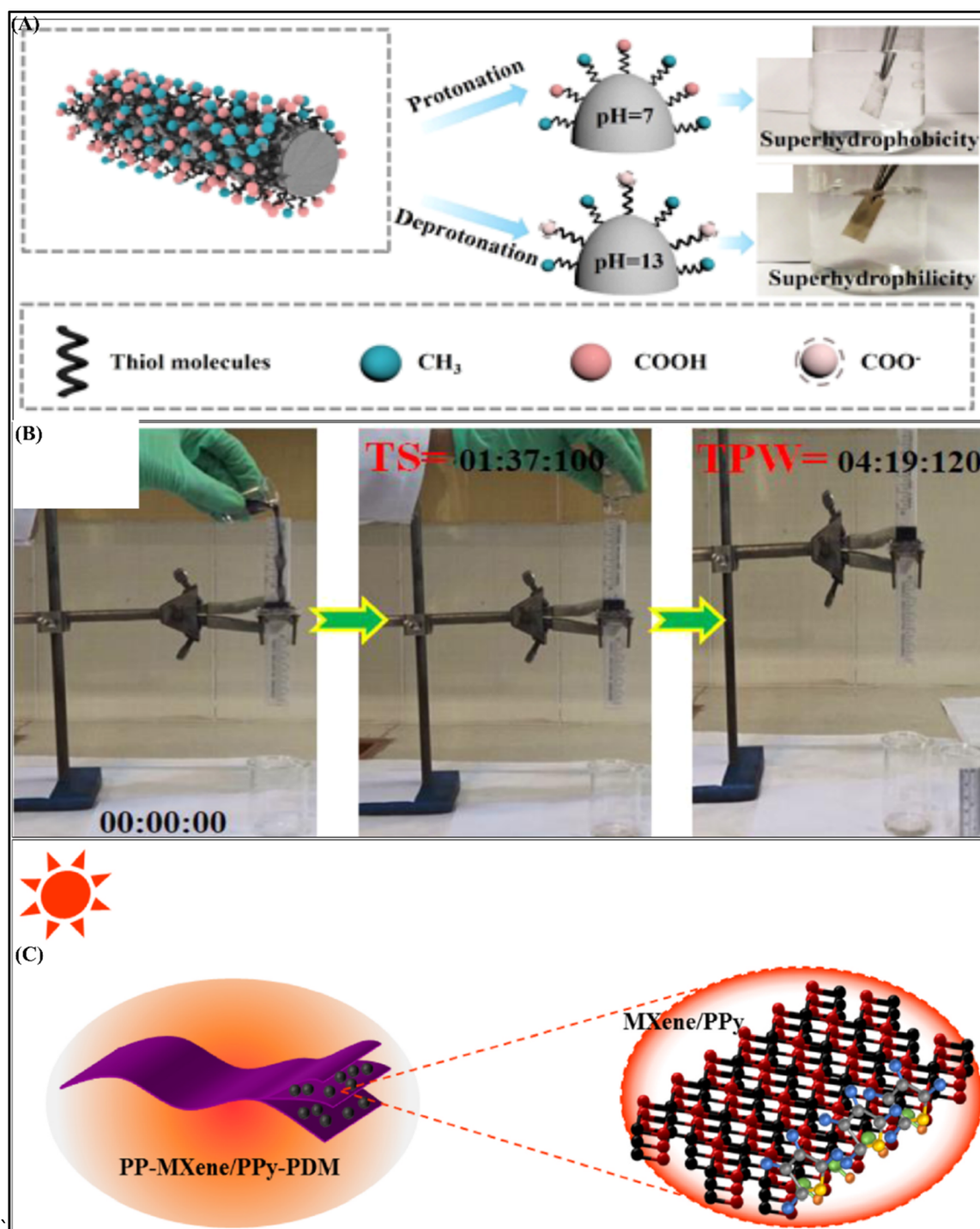


Fig. 10 (A) Mechanism illustration of the wettability switching of the pH-responsive membrane at pH 7 and 13, reproduced with permission from ref. 86; (B) oil–water separation time, reproduced with permission from ref. 89; (C) schematic illustration of the photo thermal conversion in the PP-MXene/PPy-PDM membrane, reproduced with permission from ref. 90.



reagents' TETRA to MMSDC molar ratio was optimized to 1 : 3, as it shows a SCA of 166°, SA of 7.5°, which confirms the effective attainment of low surface energy groups and hydrophobicity on the fabric. Mechanical stability was assessed through sandpaper abrasion for 25 cycles, which shows that the WCA dropped from 166° to 151° without losing its superhydrophobicity. Additionally, it exhibits excellent self-cleaning and antifouling properties as it repels the various pollutants of organic dye, saltwater, coffee, milk, cola, and tea.

## 4. Superhydrophilic and underwater superoleophobic (SHL/UWSOB) PDA-coated textiles for oil/water separation

SHL/UWSOB textiles are superwettable textiles that display underwater oil contact angles (UWCAs) above 150° and possess a super affinity for water and will, therefore, remove water from any oil–water mixture while strongly repelling oil.<sup>114</sup> SHL/UWSOB textiles can overcome the shortcomings of the oil-removing superhydrophobic textiles which include: (1) inability to remove low-density oils and highly viscous oils from their corresponding oil/water mixtures and (2) easy fouling of the superhydrophobic textile membrane that usually results in pore blockage and loss of the separation capacity.<sup>115</sup> Superhydrophilicity is responsible for an ultra-low fouling capacity that translates to a sustained, efficient, and consistent separation capacity. Though not easy to fabricate, SHL/UWSOB textiles

are excellent materials for the easy removal of water from both surfactant-stabilized and non-surfactant-stabilized oil/water mixtures, irrespective of their viscosity or density. Many documented fabrication approaches, for SHL/UWSOB materials, involve the use of toxic fluorine-containing particles and the use of substrates sourced from non-renewable materials such as stainless steel mesh, polyvinylidene fluoride (PVDF) membranes, copper mesh, *etc.*<sup>115</sup> In comparison, woven and nonwoven textiles and fabrics are advantageous as they provide flexibility, porosity, mechanical/chemical stability, and elasticity that potentially contribute to a scalable process. The surface roughness of the superhydrophilic textiles can be increased by using various nanoparticles. However, the wettability achieved by the incorporation of these nanoparticles is usually short-lived as they are easily dislodged from such surfaces by mechanical abrasion. Therefore, polydopamine has been used in conjunction with these nanoparticles to increase the lifespan of their wettability and decrease the rate of dislodgement and the effect of abrasion. Other polymers such as chitosan, polyethyleneimine, *etc.* have been used in conjunction with polydopamine to improve the superhydrophilicity already imparted because of the presence of a high number of amine and hydroxyl functional groups on the backbone of these polymers.

### 4.1. Cotton textiles

Among the substrates used for the fabrication of SHL/UWSOB separation textiles, cotton stands out because it is sourced

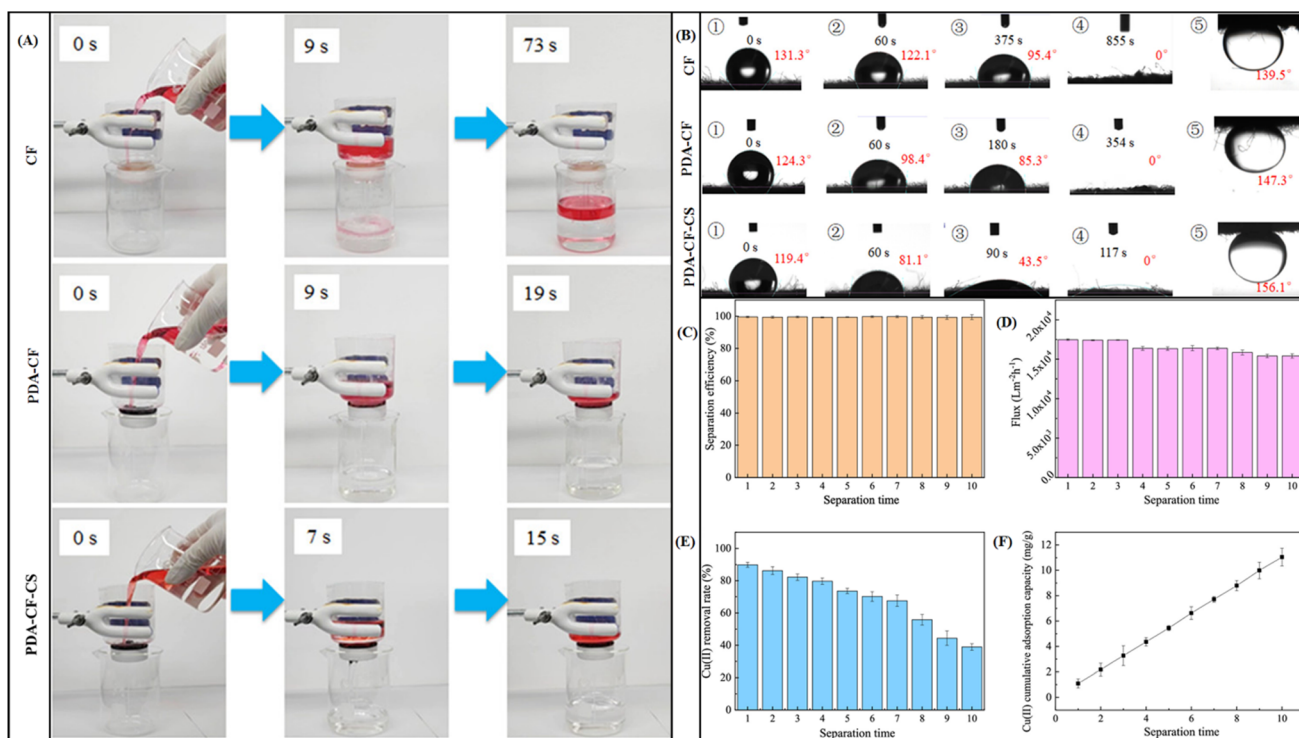


Fig. 11 Digital images showing the separation process of Cu(II)–oil–water using CF, PDA–CF, and PDA–CF–CS (A); WCA and UWOCA for CF, PDA–CF, and PDA–CF–CS (B); flux and separation efficiency (C and D); and copper adsorption capacity of PDA–CF–CS (E and F), reproduced with permission from ref. 120.



from readily available and renewable resources, is easily biodegradable, and is relatively inexpensive. Its biodegradability means that it is recyclable, which greatly reduces its contribution to the problem of environmental pollution at the end of its life cycle. Just like other textiles, cotton textiles are equally flexible and lend themselves to scalable fabrication processes. One major setback to the use of cotton fabric (CF) as a substrate is its weak adhesion to the NPs and other materials used for imparting surface roughness. Consequently, the ability of the mussel-inspired dopamine to adhere strongly to practically any surface readily solves the challenge of limited adhesion for CF. Additionally, though untreated cotton has abundant hydroxyl groups, its affinity for water is suboptimal due to the presence of non-cellulose components such as pectin, lignin, and wax.<sup>95</sup> As a result, pretreatment with ultrasonication or an alkali thermal process, or both is undertaken before coating. Micro-dissolution and coagulation have been used as an approach to improve the adhesivity of the CF-based material.<sup>116</sup> In this approach, the CF is impregnated with a dissolution solution that lightly dissolves the surface of the fabric. The multiple steps involved in this approach may prove a disadvantage. Other polymers such as polyurethane<sup>117</sup> and polyethyleneimine<sup>118</sup> have been used to improve adhesivity.

Wang and colleagues developed a SHL/UWSOB cotton fabric by using a combination of PDA and chitosan (CS) (PDA-CS-CF).<sup>115</sup> They evaluated the effect of each polymer individually and in combination on the UWOCAs and the stability of the hydrogel coat under harsh conditions. The separation efficiency for petroleum ether and soybean oil–water mixtures was above 99.5%, with a flux of 41 000 and 28 000 L m<sup>-2</sup> h<sup>-1</sup> respectively. These values persisted after 100 filtration cycles and after the PDA-CS-CF samples were subjected to ultrasonic, saltwater, alkaline, and acidic solution treatments. Likewise, Li and coworkers prepared a SHL/UWSOB cotton fabric for the dual removal of heavy metal ions and oil from artificial oily wastewater using the same CS and PDA polymers, but with a slightly different deposition method.<sup>119</sup> Polydopamine was deposited on an ultrasonically cleaned CF in an oxidative polymerization process from a solution of dopamine HCl over 24 hours to yield PDA-CF. Chitosan was subsequently deposited on the dried PDA-CF from a 1% w/v solution of chitosan in glacial acetic acid to yield PDA-CF-CS after drying. The amino groups in chitosan provided adsorption points for heavy metals and crosslinking points with the quinone structure in the polydopamine coat. Fig. 11A shows the digital images of the separation process for the copper-contaminated oil–water using CF, PDA-CF, and PDA-CF-CS. As shown in Fig. 11B, the lowest water infiltration time was 117 s for the superhydrophilic PDA-CF-CS, while the UWOCAs were 139.5°, 147.3° and 156.1° for CF, PDA-CF, and PDA-CF-CS, respectively. The UWOCAs of PDA-CF-CS decreased to 152.6° after 300 abrasion cycles of 40 cm/cycle under a 200 g weight.

The oil–water separation efficiency remained above 99% after 10 separation cycles while the water flux decreased from 17 400 L m<sup>-2</sup> h<sup>-1</sup> to 15 400 L m<sup>-2</sup> h<sup>-1</sup> by the 10th cycle (Fig. 11C and D). The copper removal efficiency was about 89% which decreased within 2 min to 67% during continuous filtration

(Fig. 11E and F). Zhong and coworkers<sup>95</sup> utilized titanium oxide NPs (due to their antibacterial, UV shielding, and hydrophilicity), polydopamine (to improve the adhesion and hydrophilicity), and (3-aminopropyl) triethoxysilane (KH550) (to improve the stability of polydopamine in an alkaline environment and additional hydration capacity), in a one-step impregnation process to prepare the SHUSO cotton fabric. The TiO<sub>2</sub> NPs and PEG were dispersed in Tris–HCl buffer to which copper sulphate, hydrogen peroxide, KH550, and dopamine were subsequently added. The CF, soaked in sodium hydroxide at 95 °C for 24 hours, was ultrasonically cleaned and dried, and then soaked in the impregnating solution. Synergistic cross-linking polymerization across the KH550, catechol group of the dopamine, and TiO<sub>2</sub> NPs ensured the firm fixation of the modification on the CF. The water spreading time of the modified CF decreased from 13.45 s for the pristine CF to 0.5 s. The UWOCAs for all the oils used was above 169°. The separation efficiency for an oil–water mixture remained above 99.99% after 50 filtration cycles and immersion in acidic, alkaline, and salt solutions. A maximum flux of 32 000 L m<sup>-2</sup> h<sup>-1</sup> was obtained that varied slightly after 3 cycles. The separation efficiency of the modified CF remained above 99.99% after being subjected to 50 abrasion cycles (20 cm per cycle) on 800-grit sandpaper under 2800 Pa pressure.

Hu *et al.*<sup>102</sup> developed the SHL/UWSOB fabric for oil–water separation and removal of dyes by a two-step process of dip-coating in poly(sodium 4-styrenesulfonate) (PSS) enveloped carbon nanotube (CNT) dispersion, followed by the subsequent *in situ* deposition of PDA. Surface roughness ( $R_a$ ) of virgin cotton was elevated from 27.005  $\mu$ m to 34.055  $\mu$ m by the incorporation of PSS and PDA nanoparticles. The attained fabric shows the separation efficiency of greater than 99.8% with an UWOCAs of 160°, which clearly reveals its super wetting ability. Besides that, it exhibits about a 97% removal rate for cationic dyes, especially methylene blue, due to the addition of porous CNTs, which provide excellent dye adsorption and hydrophilic capability for the modified fabric. Additionally, it displays a UWOCAs of >150° after exposure to the harsh conditions, *viz.* sandpaper abrasion, immersion in various organic solvents, 30% NaCl for 7 days, and immersion in aqueous solutions of various pH values of 1 to 13. The above outcomes indicated that the modified fabric has excellent stability and durability, which can be ascribed to the strong interactions among PDA, CNT, PSS and cotton fabric owing to the presence of hydrogen bonding between them.

Li and his colleagues,<sup>103</sup> developed the inexpensive and eco-friendly SHL/UWSOB fabric for oil–water separation *via* oxidative polymerization of DA on the cotton fabric and SiO<sub>2</sub> was integrated through a solution immersion process. The attained PDA/SiO<sub>2</sub>/cotton fabric reveals a UWOCAs of 159.7° with the separation efficiency of greater than 98% for crude oil/water and 99% for toluene/water. Additionally, UWOCAs are still greater than 150° after undergoing ultra-sonication (9 h), sandpaper abrasion (500 cycles), and immersion in strong acid, strong alkali, NaCl solutions (31 days), signifying that the developed cotton fabric has notable mechanical and chemical stability. It is noteworthy to mention that the deionized water can be used easily to remove the crude oil attached to the developed fabric



surface, which clearly indicates the anti-crude oil fouling property of the  $\text{SiO}_2/\text{PDA}/\text{CF}$  fabric.

#### 4.2. Other SHL/UWSOB textiles

Woven fabrics and unwoven fibers made from materials other than cotton have been investigated for the fabrication of SHL/UWSOB in different studies. At the forefront of such studies are the electrospun nanofibers made from a variety of polymers such as polyacrylonitrile (PAN)<sup>121</sup> polyacrylonitrile ether nitrile (PEN), and polyurethane (PU).<sup>122</sup> Other textiles include nonwoven fabrics such as polyester,<sup>94</sup> and nylon.<sup>99</sup> Electrospun fibers (EFs) are highly porous substrates with continuously interconnected pores and particularly offer advantages for the separation of surfactant stabilized oil–water mixtures because of their pore and diameter size that can be controlled to range from a few nanometers to micrometers.<sup>121</sup> Even though many EFs are superhydrophobic, Zhao and co-workers prepared a polydopamine functionalized SHL/UWSOB fiber using polyacrylonitrile (PAN), a superhydrophilic polymer from acrylonitrile repeating units.<sup>121</sup>

As shown in Fig. 12A, EFs were first prepared using a 10% solution of PAN in DMF and subsequently decorated with PDA NPs by immersing in a Tris–HCl buffer solution of dopamine at pH 8.5 for 7 hours. The permeation flux and the separation efficiency ranged from  $1496 \text{ L m}^{-2} \text{ h}^{-1} \text{ bar}^{-1}$  and 93.2% for  $n$ –

hexane/water emulsion to  $1570 \text{ L m}^{-2} \text{ h}^{-1} \text{ bar}^{-1}$  and 96.1% for hexadecane/water emulsion, respectively (Fig. 12B). The optical micrographs showing the emulsion before and after separation using the PAN@PDA EF for  $n$ -hexane (C1/C2), dodecane (D1/D2), and hexadecane (E1/E2) emulsions are shown in Fig. 12C–E. Fig. 12F and G depict the permeation rate for a drop of water on a pristine PAN fiber and a PAN@PDA fiber, respectively.

Li and colleagues developed a SHL/UWSOB surface on nonwoven polyester fabric by deposition of a polydopamine–polyethyleneimine (PDA–PEI) complex,<sup>94</sup> as shown in Fig. 13A. Ammonium persulphate was introduced as a superior oxidizing agent for the co-deposition reaction. The as-prepared fabric showed a UWOCA of  $165.4 \pm 1.1^\circ$ ; a SA of  $2.5 \pm 0.5^\circ$ ; an artificial oil–water separation efficiency above 99%; and a flux that ranged from  $115\,000 \text{ L m}^{-2} \text{ h}^{-1}$  to  $118\,000 \text{ L m}^{-2} \text{ h}^{-1}$ , which persisted even after 100 filtration cycles, representing capacity for continuous filtration. Furthermore, the stability of the coating to retain its separation capacity under different harsh conditions was evaluated at pH 2, 7, and 12. The UWOCA of the PDA–PEI coated textile decreased by only  $1^\circ$  under these harsh conditions.

Liu and colleagues reported the fabrication of hierarchical structures composed of silver nanoclusters on polydopamine spheres coated on a nonwoven nylon textile *via* a chemical wet

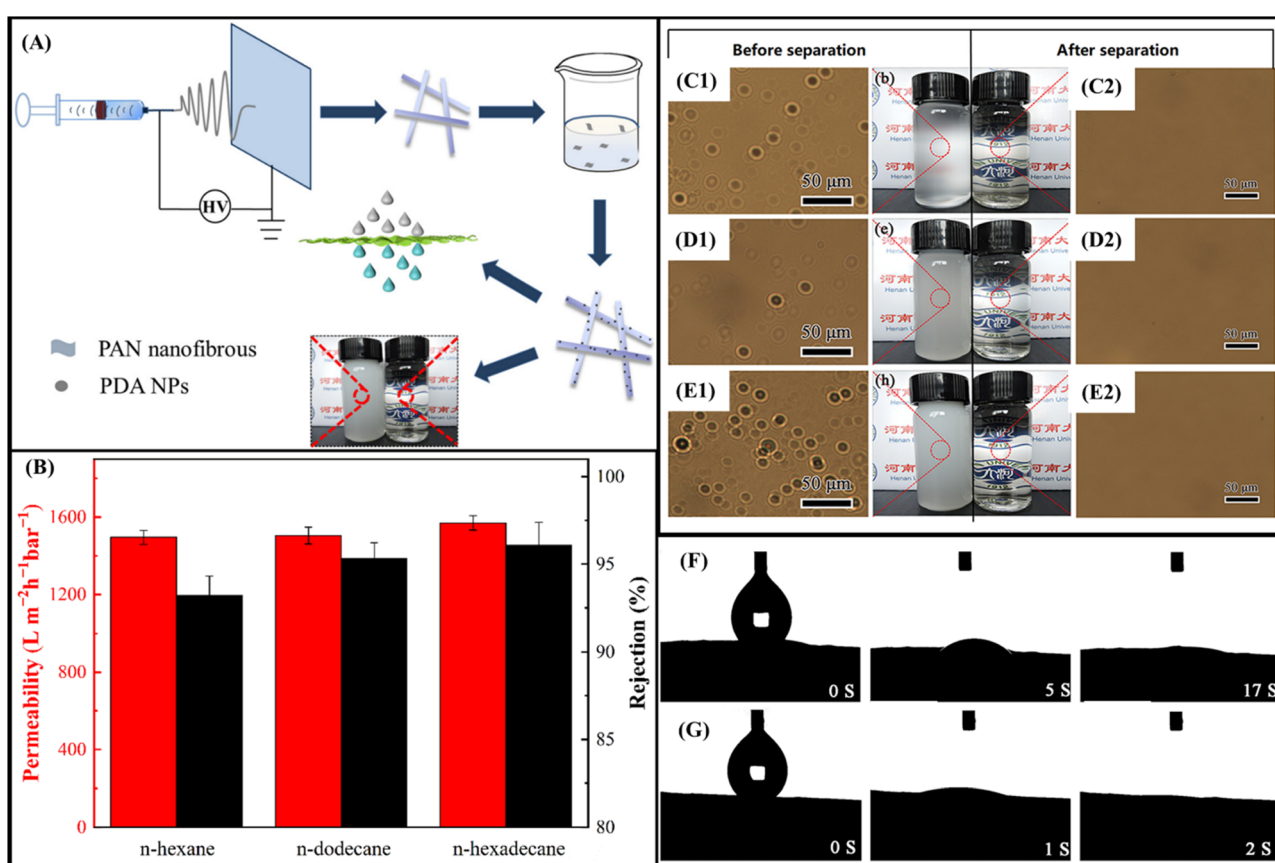


Fig. 12 Preparation process (A); permeability and separation efficiency (B); optical micrographs of  $n$ -hexane/water (C1), dodecane/water (D1), hexadecane/water (E1) emulsions and their separations (C2, D2, and E2) respectively; and spreading time of water drop on pristine PAN (F) and PAN@PDA (G), reproduced with permission from ref. 121.

reduction method<sup>99</sup> (Fig. 13B). The UWOCAs was above 150° with a diesel–water emulsion separation efficiency above 98% that persisted after 12 filtration cycles. The modified SHL/UWSOB membrane equally exhibited antibacterial activity against *E. coli* and demonstrated the catalytic reduction of methylene blue in the oil/water emulsion.

Huang and colleagues prepared a strong, electrically conductive, and stretchable SHL/UWSOB from electrospun polyurethane (PU) by first coating acidified carbon nanotubes on the electrospun PU.<sup>122</sup> Subsequently, PDA@PU/ACNTs were prepared by coating PDA onto the PU/ACNT composite, as shown in Fig. 14A. The water contact angle of PDA@PU/ACNTs

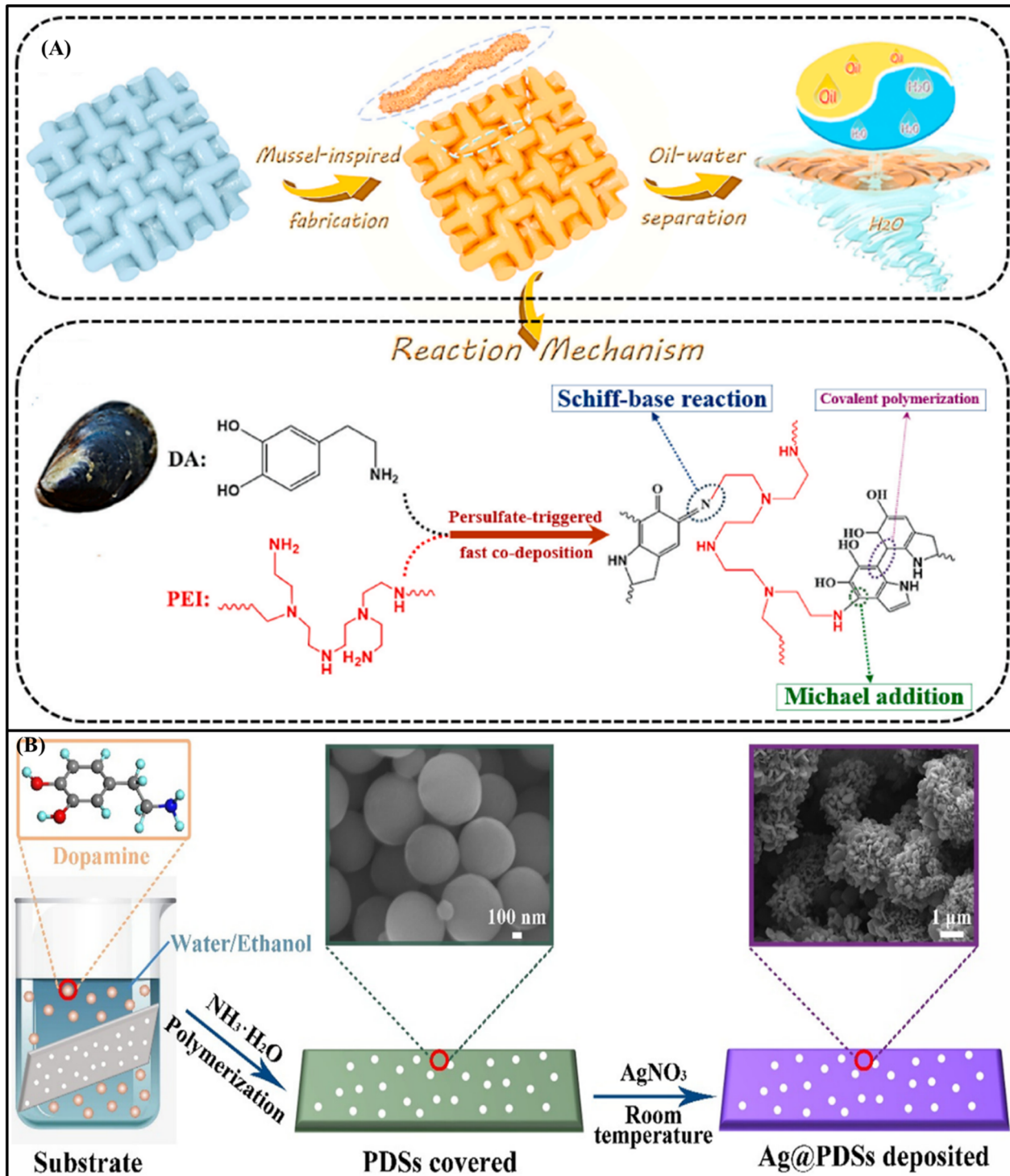


Fig. 13 Schematic illustration of (A) the mussel-inspired coating for design of superhydrophilic non-woven fabric membranes and its proposed reaction mechanism of fast codeposition of dopamine (DA) and PEI triggered by persulfate via Michael addition and Schiff-base reactions, reproduced with permission from ref. 94; (B) synthesis of the Ag@PDS deposited membrane, reproduced with permission from ref. 99.



rapidly decreased from  $62^\circ$  to  $0^\circ$  in less than 30 s with UWOCAs above  $150^\circ$ . The flux ranged from  $4108 \text{ L m}^{-2} \text{ h}^{-1}$  to  $7240 \text{ L m}^{-2} \text{ h}^{-1}$  for heptane and cyclohexane in water emulsions, respectively. The separation efficiency remained above 99.7% even after 10 cyclic separations, though the flux decreased to  $3608 \text{ L m}^{-2} \text{ h}^{-1}$ .<sup>122</sup> Zhang and colleagues exploited the synergy between an electrospun poly (arylene ether nitrile) (PEN) and polydopamine-coated hexagonal boron nitride (h-BN)

nanosheets to fabricate a thermo-stable, corrosion-resistant composite SHL/UWSOB double-layered membrane.<sup>123</sup> They found that the superhydrophilicity represented by the WCA was associated with the h-BN-PDA content and decreased from  $122^\circ$  to  $0^\circ$  as the h-BN-PDA content increased to 0.75 mg. The UWOCAs for different oils evaluated was below  $150^\circ$  and hence below the ideal value for underwater superoleophobicity. The separation flux for hexane–water emulsion was negatively

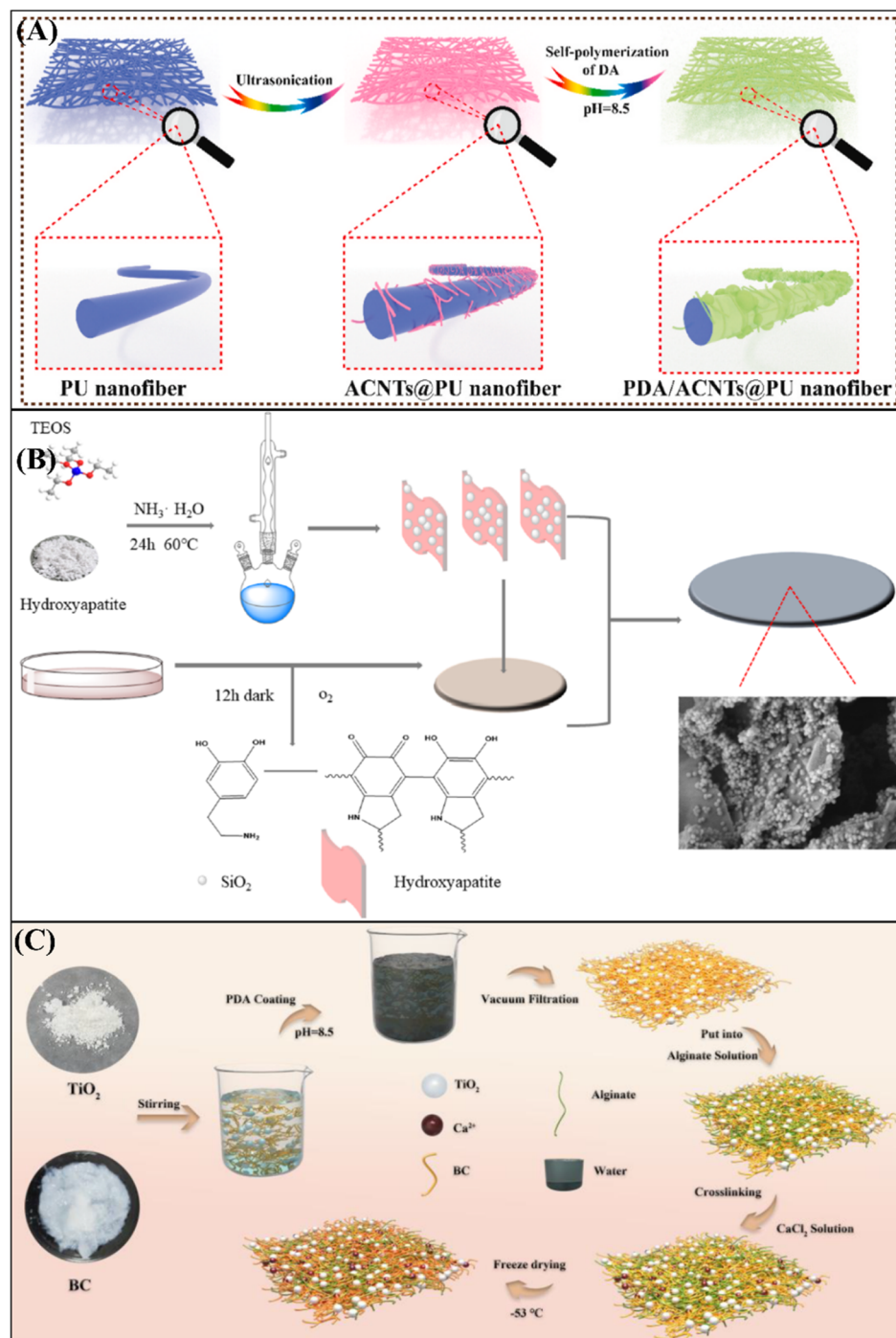


Fig. 14 Schematic illustration for preparation of composite membranes: (A) PDA@PU/ACNTs, reproduced with permission from ref. 122. (B) HAP/SiO<sub>2</sub>/PDA, reproduced with permission from ref. 100. (C) Bacterial cellulose/PDA/TiO<sub>2</sub>, reproduced with permission from ref. 101.



affected by the h-BN-PDA content decreasing from  $1894.55\text{ L m}^{-2}\text{ h}^{-1}$  to  $1274.51\text{ L m}^{-2}\text{ h}^{-1}$  as the content increased from 0 mg to 0.75 mg, though the separation efficiency at this point was still above 99%. Likewise, the flux of the composite membrane decreased to  $588\text{ L m}^{-2}\text{ h}^{-1}$  after 10 filtration cycles for the emulsion, but remained above  $8400\text{ L m}^{-2}\text{ h}^{-1}$  for the oil–water. Overall, the separation efficiency remained above 99% through the 10 cycles. The resistance of the composite membrane to elevated temperatures in the oven was confirmed by the unchanged flux and separation efficiency of the membrane while it showed a decrease in wettability when exposed to additional corrosive solutions at elevated temperature ( $65\text{ }^{\circ}\text{C}$ ).<sup>96</sup>

Wang *et al.*<sup>100</sup> developed the SHL/UWSOB composite membrane based on micro cellulose ester through *in situ* process for synthesizing nano materials and vacuum filtration for membranes (Fig. 14B). Hydrophilicity was achieved by the addition of  $\text{SiO}_2$  nano materials on hydroxyapatite (HAP) with the synergistic effect of polydopamine. The prepared composite membrane of HAP/ $\text{SiO}_2$ /PDA shows the high-water permeability flux and a separation efficiency of 90.90% over a wide range of light to heavy oils. The obtained UWOCA ranges from  $149.75 \pm 80.42^{\circ}$  to  $155.265 \pm 1.902^{\circ}$  for all the prepared membranes, and the WCA was decreased from  $27.63 \pm 0.997^{\circ}$  to  $11.07 \pm 0.169^{\circ}$  due to the influence of TEOS, which exhibits the wettability attributes of the composite membranes. Mechanical durability was assessed by the scratch test through knife and finger, which exhibits a UWOCA of  $>150^{\circ}$  and a separation efficiency of  $>98\%$ . Furthermore, it shows a UWOCA of  $>140^{\circ}$  after being immersed separately in corrosive solutions of acidic/alkaline and salt for 3 days, which reveals the endurance of underwater superoleophobic properties.

Cui and colleagues<sup>101</sup> fabricated the non-toxic, low cost and environmentally friendly composite membrane based on bacterial cellulose, which can decay organic pollutants under

ultraviolet light. They employed PDA as an anchoring substance for  $\text{TiO}_2$  nanoparticles on the surface and cross-linked with sodium alginate by vacuum assisted filtration and freeze-drying techniques (Fig. 14C). The prepared membrane (bacterial cellulose/PDA/ $\text{TiO}_2$ ) shows the separation efficiency of  $>99\%$  for low and heavy viscous oil–water mixtures with a WCA of  $0^{\circ}$  and a UWOCA of  $156.5^{\circ}$ . It shows the effective attainment of superhydrophilic and underwater superoleophobic properties due to the addition of  $\text{TiO}_2$  and sodium alginate. As the addition of sodium alginate assists in making the membrane with a porous structure, which increases the water flux of the membrane. However, after repeated separation of the oil–water mixture, the WCA was dropped to  $125.6^{\circ}$ , and it was regenerated to  $154^{\circ}$  with the aid of UV radiation. Additionally, antifouling and extended service life of the membrane was attained by the addition of  $\text{TiO}_2$ , which serves as a catalyst in decomposing the organic pollutants under UV irradiation.

## 5. Emulsion separation

As illustrated in Fig. 15, emulsions can be separated through two main mechanisms: size-sieving or demulsification.<sup>124,125</sup> In size-sieving, the pore size of the material must be equal to or smaller than the emulsified droplets (Fig. 15a). However, smaller pores can hinder permeation flux, resulting in lower separation efficiency compared to membranes used for immiscible oil/water separation. In contrast, membranes designed for demulsification typically have moderate pore sizes, allowing for higher permeation flux and improved separation performance<sup>126,127</sup> (Fig. 15b). In principle, water-in-oil (w/o) emulsions are separated using superhydrophobic membranes, whereas oil-in-water (o/w) emulsions require superhydrophilic and underwater superoleophobic membranes.<sup>34</sup> The separation of emulsified oil/water mixtures is still a challenging industrial concern due to the stability of the surfactant-stabilized w/o and/

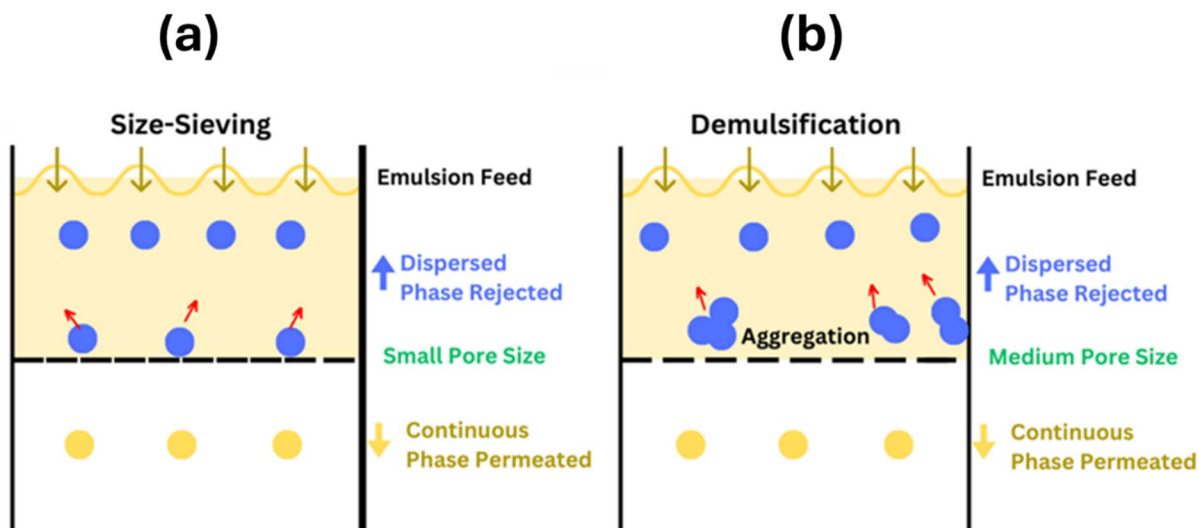


Fig. 15 Schematic illustration for the separation mechanisms of emulsified oil/water mixtures: (a) size-sieving mechanism, and (b) demulsification mechanism, reproduced with permission from ref. 34.



or o/w emulsions as well as their tiny droplet size ( $<2\text{ }\mu\text{m}$ ).<sup>128,129</sup> Therefore, advanced ultrafiltration (UF) and microfiltration (MF) membranes have been effectively used to separate various types of emulsified oil/water mixtures through the size-sieving mechanism.<sup>130,131</sup> In contrast, superwetting textiles with the macroporous structure (*i.e.* pore size of hundreds of microns) have been utilized for the separation of emulsified oil/water mixtures through a demulsification pathway.<sup>26,132–135</sup>

There are limited reports that have utilized polydopamine-coated textiles for the separation of emulsified oil/water mixtures. Li *et al.* developed a switchable cotton fabric for oil–water separation and water purification.<sup>136</sup> To create a rough micro–nano scale surface with high surface energy—allowing selective wetting and repelling of immiscible media—they incorporated polydopamine and  $\text{NiFe}_2\text{O}_4$  nanoparticles. Surface morphology and compositional analysis confirmed a uniform  $\text{NiFe}_2\text{O}_4$  coating on the cotton fabric. The modified fabric exhibited a water contact angle (WCA) of  $145^\circ$  in oil and an oil contact angle (OCA) of  $153^\circ$  in water, demonstrating its superamphiphilic nature in air and lyophobic properties. When mounted between two vertical glass tubes for emulsion separation, the fabric effectively separated both oil-in-water and water-in-oil emulsions. Optical microscopy confirmed the absence of internal-phase droplets in the collected filtrates, achieving a separation flux of approximately  $300\text{ L m}^{-2}\text{ h}^{-1}$  by gravity with a rejection ratio of about 99%. Similar results were observed for other surfactant-stabilized emulsions, including SDS-stabilized hexadecane-in-water, diesel-in-water, and Span 80-stabilized water-in-hexane and water-in-chloroform. Cycle performance tests using SDS-stabilized toluene-in-water and water-in-dichloromethane emulsions showed that the fabric retained stable separation efficiency even after washing with water or dichloromethane. Although oil/water flux gradually decreased over time due to cake formation on the surface, the fabric exhibited antifouling properties, ensuring sustained separation performance. Additionally, its porous structure enabled the adsorption of methylene blue, highlighting its potential for water treatment applications.

Gan *et al.* utilized polydopamine as a binder and reducing agent for the *in situ* deposition of silver (Ag) nanoparticles onto a textile surface.<sup>137</sup> This was followed by an immersion step in PFOA-Na ethanol solution to achieve a slippery oil-repellent state, creating a superhydrophobic/superhydrophilic (SHB/SHL) Ag/polydopamine-coated textile (Ag/PDA@textile). The incorporation of Ag nanoparticles endowed the textile with photocatalytic and antibacterial properties, enabling its application for dye removal from water and the inhibition of bacterial growth. The modified textile exhibited superhydrophilic and superoleophobic characteristics in air, with an oil contact angle (OCA) greater than  $150^\circ$  and a sliding angle (SA) of less than  $9^\circ$ . When wetted with water, it displayed an OCA of  $50.1^\circ$ , allowing oil to flow smoothly across its water-wetted surface due to the water lubricant's fluidity. Notably, even after being submerged in oil for a day, the water-wetted textile retained its oil-repelling properties, demonstrating excellent anti-oil-fouling capabilities. Oil–water separation tests revealed a high-water permeation flux of  $1502\text{ L m}^{-2}\text{ h}^{-1}\text{ bar}^{-1}$  and

a separation efficiency exceeding 99% for toluene–hot water mixtures at  $80.5\text{ }^\circ\text{C}$ . Comparative microscopy images before and after emulsion separation (Tween 80-stabilized toluene-in-water) further highlighted its effectiveness in separating o/w emulsions. Additionally, Ag/PDA@textile demonstrated the ability to separate immiscible oil/oil mixtures with varying polarities, showing a strong affinity for high-polarity oils while repelling low-polarity oils.

## 6. Conclusions and perspectives

Polydopamine (PDA) coatings are well known for their universal, material-independent application on various solid substrates. They can effectively cover target material surfaces, even in cases of low intermolecular interactions. Over the past decade, PDA has been widely used to fabricate superwetting textiles and fabrics through simple, sustainable, and versatile synthetic pathways. The use of PDA coatings offers several advantages in fabricating superwetting textiles, including inherent hydrophilicity, enhanced adhesion and roughness of the coated surfaces, potential for *in situ* post-functionalization (*e.g.*, incorporating nanoparticles using PDA as a reducing agent), good chemical durability, intrinsic antibacterial properties, and biodegradability. Additionally, the strong adhesion properties of PDA coatings facilitate the incorporation of various low-surface-energy materials (*e.g.*, alkyl thiols, alkylamines, and fatty acids) and metal nanoparticles (*e.g.*, silver NPs) through ionic and/or covalent interactions. This improved adhesion contributes to the overall durability and recyclability of superwetting textiles. Furthermore, PDA coatings support the development of smart, multifunctional superwetting textiles with features such as self-healing and UV resistance.

Despite these advantages, conventional PDA coating strategies face challenges such as time consumption and poor controllability. These issues arise from the slow kinetics of DA polymerization and inevitable aggregation, which limit practical manufacturing processes and hinder precise tuning of surface characteristics.<sup>138</sup> As shown in Tables 1 and 2, the first challenge is related to the fabrication process, which is time-consuming. Most reported studies employ *in situ* auto-oxidative polymerization using a Tris buffer (pH = 8.5/O<sub>2</sub>), requiring long deposition periods ( $\approx 24$  hours) for a PDA coating. The second challenge is related to the development of efficient strategies for restricting DA polymerization exclusively to the material's surface, minimizing waste caused by excessive self-polymerization in the solution. The first and the second challenges can be addressed by employing a direct and rapid dip-coating strategy of the textiles/fabrics in pre-polymerized polydopamine dispersions.<sup>139</sup> In this approach, nanoparticles can be added to the polydopamine dispersion, or the dispersion itself can be prepared in the presence of the desired nanoparticles. The dip-coating method also helps to reduce the excess PDA waste. However, this proposed technique may influence the final wetting behaviour of the modified textiles due to PDA's inherent hydrophilicity and adhesion properties. To optimize adhesion, the number of dip-coating cycles can be adjusted. Additionally, post-functionalization can still be



performed to modify the surface energy properties of polydopamine-coated textiles compared to those of uncoated textiles.

Another solution that enables rapid polydopamine coatings is the use of an effective oxidizing agent and/or auxiliary oxidizing agents (*i.e.* redox system) that accelerate the rate of oxidative polymerization. As can be inferred from Tables 1 and 2, only a limited number of studies have utilized the rapid oxidation procedures during the fabrication process. Hence, this area is an active research area that has not yet been fully explored to accelerate the polydopamine coating and shorten the overall fabrication time. In this respect, there are numerous redox systems that have been reported for the rapid polymerization of polydopamine, including  $\text{Cu}^{2+}/\text{H}_2\text{O}_2$ ,<sup>140,141</sup>  $\text{Fe}^{3+}/\text{H}_2\text{O}_2$ ,<sup>142</sup>  $\text{Fe}^{2+}$ ,<sup>143</sup> ozone ( $\text{O}_3$ ),<sup>144</sup> and sodium periodate ( $\text{NaIO}_4$ ).<sup>145</sup> PDA exhibits good anticorrosion resistance in neutral and acidic environments but may partially degrade under alkaline conditions ( $\text{pH} > 12$ ). In practical applications, pretreating water effluent to achieve a neutral pH can help extend the lifespan of PDA-coated membranes by avoiding extreme pH conditions. Notably, even state-of-the-art biodegradable superwetting crosslinked membranes degrade easily under alkaline conditions (1 M NaOH).<sup>131</sup> Nevertheless, applying a secondary protective coating (*e.g.*, PDMS) can enhance the chemical durability of PDA-coated textiles, albeit at the expense of increased fabrication cost and time. Additionally, the mechanical durability and relatively high cost of PDA coatings must be carefully considered in future studies.<sup>46</sup>

From the perspective of oil/water separation, future research should focus on developing faster, cost-effective, one-step fabrication methods and scaling up the production of PDA-coated superwetting textiles. The use of polydopamine nanoparticles (*e.g.* synthesized in the ethanol/water mixture) is expected to improve the superwetting performance of the coated textiles due to the improved surface roughness.<sup>67</sup> Future studies should also emphasize the separation of both stratified and emulsified oil/water mixtures, including viscous crude oils and water-in-oil (w/o) and oil-in-water (o/w) emulsions. Another direction that has emerged is the application of polydopamine-coated materials for water purification and decontamination (*e.g.* removal of dyes, toxic metal ions, *etc.*).<sup>146–151</sup> Hence, dopamine-coated fabrics could be utilized for both oil/water separation and decontamination due to the potential adsorption of polydopamine to diverse arrays of toxic organic and inorganic contaminants through different ionic interactions. This can be achieved with/without the presence of photocatalysts immobilized on the surface of the coated textiles.<sup>152</sup> Besides the rapid degradation of the organic contaminants, the embedded photocatalysts are expected to improve the self-cleaning and antifouling performance of the polydopamine-coated textiles.

## Data availability

This is a review article. All the presented data are based on the literature reports.

## Author contributions

Conceptualization: Nedal Abu-Thabit; visualization: Abdul Kalam Azad, Mahmoud Abu Elella, and Nedal Abu-Thabit; writing—original draft: Abdul Kalam Azad, Mahmoud Abu Elella, and Nedal Abu-Thabit; writing—review & editing: Nedal Abu-Thabit.

## Conflicts of interest

The authors declare that they have no conflict of interest.

## References

- W. F. Elmobarak, B. H. Hameed, F. Almomani and A. Z. Abdullah, A Review on the Treatment of Petroleum Refinery Wastewater Using Advanced Oxidation Processes, *Catalysts*, 2021, **11**(7), 782.
- M. Manickam, B. Giridharan and M. S. K. Kumar, Microbial Diversity and Physio-Chemical Characterization and Treatment of Textiles Effluents, in *Environmental Degradation: Challenges and Strategies for Mitigation*, Springer, 2022, pp. 253–266.
- S. Garg, Z. Z. Chowdhury, A. N. M. Faisal, N. P. Rumjit and P. Thomas, Impact of Industrial Wastewater on Environment and Human Health, in *Advanced Industrial Wastewater Treatment and Reclamation of Water*, Springer, 2022, pp. 197–209.
- S. Malik, S. Kishore, S. Prasad and M. P. Shah, A comprehensive review on emerging trends in industrial wastewater research, *J. Basic Microbiol.*, 2022, **62**(3–4), 296–309.
- S. Garg, Industrial wastewater: Characteristics, treatment techniques and reclamation of water, in *Advanced Industrial Wastewater Treatment and Reclamation of Water*, Springer, 2022, pp. 1–23.
- M. S. M. Mansour, H. I. Abdel-Shafy and A. M. Ibrahim, Petroleum wastewater: Environmental protection, treatment, and safe reuse: An overview, *J. Environ. Manage.*, 2024, **351**, 119827.
- L. M. T. M. Oliveira, J. Saleem, A. Bazargan, J. L. d. S. Duarte, G. McKay and L. Meili, Sorption as a rapidly response for oil spill accidents: a material and mechanistic approach, *J. Hazard. Mater.*, 2021, **407**, 124842.
- H. Kim, G. Zhang, T. C. M. Chung and C. Nam, A Role for Newly Developed Sorbents in Remediating Large-Scale Oil Spills: Reviewing Recent Advances and Beyond, *Adv. Sustainable Syst.*, 2021, 2100211.
- S. Bhattacharjee and T. Dutta, An overview of oil pollution and oil-spilling incidents, *Advances in Oil-Water Separation*, 2022, pp. 3–15.
- S. Dey, A. Das, K. Mallick, A. Sahu and A. P. Das, Environmental Petroleum Waste: Pollution, Toxicity, Sustainable Remediation, in *Impact of Petroleum Waste on Environmental Pollution and its Sustainable Management through Circular Economy*, Springer, 2024, pp. 159–175.



11 C. K. Abdallah, K. A. Mourad and S. J. Cobbina, *Advanced Water Pollution Control Strategies: A Systematic Review*, 2022.

12 K. Abuhasel, M. Kchaou, M. Alquraish, Y. Munusamy and Y. T. Jeng, Oily wastewater treatment: overview of conventional and modern methods, challenges, and future opportunities, *Water*, 2021, **13**(7), 980.

13 A. Dhaka and P. Chattopadhyay, A review on physical remediation techniques for treatment of marine oil spills, *J. Environ. Manage.*, 2021, **288**, 112428.

14 A. D. M. d. Medeiros, C. J. G. d. Silva Jr, J. D. P. d. Amorim, I. J. B. Durval, A. F. d. S. Costa and L. A. Sarubbo, Oily Wastewater Treatment: Methods, Challenges, and Trends, *Processes*, 2022, **10**(4), 743.

15 Y. Xin, B. Qi, X. Wu, C. Yang and B. Li, Different types of membrane materials for oil-water separation: Status and challenges, *Colloids Interface Sci. Commun.*, 2024, **59**, 100772.

16 J. Yu, C. Cao and Y. Pan, Advances of Adsorption and Filtration Techniques in Separating Highly Viscous Crude Oil/Water Mixtures, *Adv. Mater. Interfaces*, 2021, **8**, 2100061.

17 M. Alshabib, U. Baig and M. A. Dastageer, Superhydrophilic and underwater super-oleophobic membranes with photocatalytic self-cleaning properties for highly efficient oil-water separation: A review, *Desalination*, 2024, 118019.

18 Z. Liu, Y. Si, C. Yu, L. Jiang and Z. Dong, Bioinspired superwetting oil-water separation strategy: toward the era of openness, *Chem. Soc. Rev.*, 2024, **53**(20), 10012–10043.

19 L. Qiu, Y. Sun and Z. Guo, Designing novel superwetting surfaces for high-efficiency oil-water separation: Design principles, opportunities, trends and challenges, *J. Mater. Chem. A*, 2020, **8**, 16831–16853.

20 Q. Fan, T. Lu, Y. Deng, Y. Zhang, W. Ma, R. Xiong, *et al.*, Bio-based materials with special wettability for oil-water separation, *Sep. Purif. Technol.*, 2022, 121445.

21 X. Jiang, F. Yang and Z. Guo, Superwetting surfaces for filtration separation of high-viscosity raw petroleum/water mixtures, *J. Mater. Chem. A*, 2022, **10**(27), 14273–14292.

22 Y. Y. Quan, Z. Chen, Y. Lai, Z. S. Huang and H. Li, Recent advances in fabricating durable superhydrophobic surfaces: A review in the aspects of structures and materials, *Mater. Chem. Front.*, 2021, **5**, 1655–1682.

23 H. Bai, C. Song, L. Zheng, T. Shen, X. Meng and J. Ma, Overview of rough surface construction technology for cotton fabrics used in oil/water separation, *RSC Sustainability*, 2025, **3**(2), 676–697.

24 H. Guo, J. Yang, T. Xu, W. Zhao, J. Zhang, Y. Zhu, *et al.*, A Robust Cotton Textile-Based Material for High-Flux Oil-Water Separation, *ACS Appl. Mater. Interfaces*, 2019, **11**, 13704–13713.

25 N. Forsman, L. S. Johansson, H. Koivula, M. Tuure, P. Kääriäinen and M. Österberg, Open coating with natural wax particles enables scalable, non-toxic hydrophobation of cellulose-based textiles, *Carbohydr. Polym.*, 2020, **227**, 115363.

26 M. H. Abu Elella, N. Y. Abu-Thabit, O. J. Uwaezuoke and A. K. Azad, Superwetting cotton textiles for separation of oil/water mixtures, *Cellulose*, 2023, 1–36.

27 N. Y. Abu-Thabit, O. J. Uwaezuoke and M. H. A. Elella, Superhydrophobic nanohybrid sponges for separation of oil/water mixtures, *Chemosphere*, 2022, **294**, 133644.

28 E. K. Sam, J. Liu and X. Lv, Surface Engineering Materials of Superhydrophobic Sponges for Oil/Water Separation: A Review, *Ind. Eng. Chem. Res.*, 2021, **60**(6), 2353–2364.

29 P. Yi, H. Hu, W. Sui, H. Zhang, Y. Lin and G. Li, Thermoresponsive Polyurethane Sponges with Temperature-Controlled Superwettability for Oil/Water Separation, *ACS Appl. Polym. Mater.*, 2020, **2**(5), 1764–1772.

30 P. Cherukupally, W. Sun, A. P. Y. Wong, D. R. Williams, G. A. Ozin, A. M. Bilton, *et al.*, Surface-engineered sponges for recovery of crude oil microdroplets from wastewater, *Nat. Sustainability*, 2020, **3**(2), 136–143.

31 M. Zhu, Y. Liu, M. Chen, Z. Xu, L. Li and Y. Zhou, Metal mesh-based special wettability materials for oil-water separation: A review of the recent development, *J. Pet. Sci. Eng.*, 2021, **205**, 108889.

32 Y. Wang, Y. Feng, M. Zhang, C. Huang and J. Yao, A green strategy for preparing durable underwater superoleophobic calcium alginate hydrogel coated-meshes for oil/water separation, *Int. J. Biol. Macromol.*, 2019, **136**, 13–19.

33 L. Qiu, J. Zhang, Z. Guo and W. Liu, Asymmetric superwetting stainless steel meshes for on-demand and highly effective oil-water emulsion separation, *Sep. Purif. Technol.*, 2021, **273**, 118994, DOI: [10.1016/j.seppur.2021.118994](https://doi.org/10.1016/j.seppur.2021.118994).

34 N. Y. Abu-Thabit, M. H. A. Elella, A. K. Azad, E. Ratemi and A. S. Hakeem, Superwetting metal mesh membranes for oil/water separation: A comprehensive review, *Sep. Purif. Technol.*, 2025, 132016.

35 N. Zhang, X. Yang, Y. Wang, Y. Qi, Y. Zhang, J. Luo, *et al.*, A review on oil/water emulsion separation membrane material, *J. Environ. Chem. Eng.*, 2022, 107257.

36 S. Zarghami, T. Mohammadi and M. Sadrzadeh, Superhydrophobic/Superhydrophilic Polymeric Membranes for Oil/Water Separation, in *Oil-Water Mixtures and Emulsions, Volume 1: Membrane Materials for Separation and Treatment*, ACS Publications, 2022, pp. 119–184.

37 E. S. Dmitrieva, T. S. Anokhina, E. G. Novitsky, V. v Volkov, I. L. Borisov and A. v Volkov, Polymeric Membranes for Oil-Water Separation: A Review, *Polymers*, 2022, **14**(5), 980.

38 X. Yu, J. Ji, Q. Y. Wu and L. Gu, Direct-coating of cellulose hydrogel on PVDF membranes with superhydrophilic and antifouling properties for high-efficiency oil/water emulsion separation, *Int. J. Biol. Macromol.*, 2024, **256**, 128579.

39 C. J. Lv, B. Hao, A. Yasin, X. Yue and P. C. Ma, H<sub>2</sub>O<sub>2</sub>-assisted preparation of superhydrophilic polyacrylonitrile fabric and its application for the separation of oil/water mixture, *Colloids Surf. A*, 2022, **646**, 129004.



40 W. Zhou, Y. Zhang, S. Du, X. Chen, K. Qi, T. Wu, *et al.*, Superwettable Amidoximed Polyacrylonitrile-Based Nanofibrous Nonwovens for Rapid and Highly Efficient Separation of Oil/Water Emulsions, *ACS Appl. Polym. Mater.*, 2021, **3**(6), 3093–3102.

41 C. Zhu, W. Jiang, J. Hu, P. Sun, A. Li and Q. Zhang, Polylactic acid nonwoven fabric surface modified with stereocomplex crystals for recyclable use in oil/water separation, *ACS Appl. Polym. Mater.*, 2020, **2**(7), 2509–2516.

42 X. Yue, Z. Li, T. Zhang, D. Yang and F. Qiu, Design and fabrication of superwetting fiber-based membranes for oil/water separation applications, *Chem. Eng. J.*, 2019, **364**, 292–309.

43 N. Abu-Thabit, A. K. Azad, K. Mezghani, A. Hakeem, D. Qasem, S. Akhtar, *et al.*, Facile and Green Fabrication of Superhydrophobic Polyacrylonitrile Nonwoven Fabric with Iron Hydroxide Nanoparticles for Efficient Oil/Water Separation, *ACS Appl. Polym. Mater.*, 2022, **4**, 8450–8460.

44 H. Bai, C. Song, L. Zheng, T. Shen, X. Meng and J. Ma, Overview of rough surface construction technology for cotton fabrics used in oil/water separation, *RSC Sustainability*, 2025, **3**(2), 676–697.

45 J. Zhang, B. Li, L. Wu and A. Wang, Facile preparation of durable and robust superhydrophobic textiles by dip coating in nanocomposite solution of organosilanes, *Chem. Commun.*, 2013, **49**(98), 11509–11511.

46 M. Saraf, Prateek, R. Ranjan, B. Balasubramaniam, V. K. Thakur and R. K. Gupta, Polydopamine-enabled biomimetic surface engineering of materials: New insights and promising applications, *Adv. Mater. Interfaces*, 2024, **11**(6), 2300670.

47 J. Lim, S. Zhang, J. M. Heo, M. C. Dickwella Widanage, A. Ramamoorthy and J. Kim, Polydopamine adhesion: catechol, amine, dihydroxyindole, and aggregation dynamics, *ACS Appl. Mater. Interfaces*, 2024, **16**(24), 31864–31872.

48 J. L. Carter, C. A. Kelly and M. J. Jenkins, Enhanced adhesion of PEDOT: PSS to substrates using polydopamine as a primer, *Polym. J.*, 2024, **56**(2), 115–120.

49 S. Eom, H. K. Park, J. Park, S. Hong and H. Lee, Recent progress on polydopamine surface chemistry, *J. Adhes.*, 2018, **19**(1), 19–29.

50 J. H. Ryu, P. B. Messersmith and H. Lee, Polydopamine surface chemistry: a decade of discovery, *ACS Appl. Mater. Interfaces*, 2018, **10**(9), 7523–7540.

51 H. A. Lee, Y. Ma, F. Zhou, S. Hong and H. Lee, Material-independent surface chemistry beyond polydopamine coating, *Acc. Chem. Res.*, 2019, **52**(3), 704–713.

52 J. Liebscher, Chemistry of polydopamine—scope, variation, and limitation, *Eur. J. Org. Chem.*, 2019, **2019**(31–32), 4976–4994.

53 R. Lakshminarayanan, S. Madhavi and C. P. C. Sim, Oxidative polymerization of dopamine: a high-definition multifunctional coatings for electrospun nanofibers—an overview, *Dopamine-Health and Disease*, 2018, pp. 113–132.

54 J. Zhu, M. T. Tsehaye, J. Wang, A. Uliana, M. Tian, S. Yuan, *et al.*, A rapid deposition of polydopamine coatings induced by iron (III) chloride/hydrogen peroxide for loose nanofiltration, *J. Colloid Interface Sci.*, 2018, **523**, 86–97.

55 N. Y. Abu-Thabit, Chemical oxidative polymerization of polyaniline: A practical approach for preparation of smart conductive textiles, *J. Chem. Educ.*, 2016, **93**(9), 1606–1611.

56 N. Y. Abu-Thabit, Nanomaterials for flexible transparent conductive films and optoelectronic devices, in *Advances in Smart Coatings and Thin Films for Future Industrial and Biomedical Engineering Applications*, Elsevier, 2020, pp. 619–643.

57 N. Y. Abu-Thabit, Electrically conducting polyaniline smart coatings and thin films for industrial applications, in *Advances in Smart Coatings and Thin Films for Future Industrial and Biomedical Engineering Applications*, Elsevier, 2020, pp. 585–617.

58 N. Abu-Thabit, Y. Umar, E. Ratemi and A. Ahmad, Polyaniline-Coated Polysulfone Membranes as Flexible Optical pH Sensors, in *Proceedings of the 2nd International Electronic Conference on Sensors and Applications*, Basel, Switzerland, 2015, pp. 15–30.

59 N. Abu-Thabit and Y. Umar, Electrically conductive polyacrylamide-polyaniline superabsorbing polymer hydrogels, in *1st International Electronic Conference on Materials (ECM)*, Montreal, Canada, 2014.

60 N. Abu-Thabit, Optical Colorimetric Sensing Label for Monitoring Food Freshness, *Eng. Proc.*, 2023, **48**(1), 16.

61 K. G. Malollari, P. Delparastan, C. Sobek, S. J. Vachhani, T. D. Fink, R. H. Zha, *et al.*, Mechanical enhancement of bioinspired polydopamine nanocoatings, *ACS Appl. Mater. Interfaces*, 2019, **11**(46), 43599–43607.

62 Y. Heo, M. Ji, C. Y. Ryu, H. Kim, I. Choi, S. M. Kang, *et al.*, Structural Modifications on Dopamine Molecules toward Polydopamine Applications, *Eur. J. Org. Chem.*, 2025, **28**(2), e202401035.

63 J. Yang, R. Wang, X. Zhang, F. Long, T. Zhou and L. Liu, Self-roughened superhydrophobic polydopamine coating with excellent self-cleaning, anti-corrosion, and UV shielding performances, *J. Appl. Polym. Sci.*, 2022, **139**(19), 52114.

64 H. A. Lee, E. Park and H. Lee, Polydopamine and its derivative surface chemistry in material science: a focused review for studies at KAIST, *Adv. Mater.*, 2020, **32**(35), 1907505.

65 M. Reinhardt, A. Drechsler, S. Putzke, F. Simon and C. A. Zimmerer, Bioinspired Adhesion Promoters for the Metalization of Polyethylene: A Comparison between Polydopamine and Tannic Acid, *ACS Appl. Polym. Mater.*, 2024, **6**(16), 9694–9704.

66 Y. Li, K. Yang, Z. Wang, J. Xiao, Z. Tang, H. Li, *et al.*, Rapid *in situ* deposition of iron-chelated polydopamine coating on the polyacrylamide hydrogel dressings for combined photothermal and chemodynamic therapy of skin wound infection, *ACS Appl. Bio Mater.*, 2022, **5**(9), 4541–4553.

67 J. Tian, X. Qi, C. Li and G. Xian, Mussel-inspired fabrication of an environment-friendly and self-adhesive superhydrophobic polydopamine coating with excellent mechanical durability, anti-icing and self-cleaning



performances, *ACS Appl. Mater. Interfaces*, 2023, **15**(21), 26000–26015.

68 C. H. Xue, X. Q. Ji, J. Zhang, J. Z. Ma and S. T. Jia, Biomimetic superhydrophobic surfaces by combining mussel-inspired adhesion with lotus-inspired coating, *Nanotechnology*, 2015, **26**(33), 335602.

69 Z. Wang, Y. Xu, Y. Liu and L. Shao, A novel mussel-inspired strategy toward superhydrophobic surfaces for self-driven crude oil spill cleanup, *J. Mater. Chem. A*, 2015, **3**(23), 12171–12178.

70 Y. Liu, Y. Liu, H. Hu, Z. Liu, X. Pei, B. Yu, *et al.*, Mechanically induced self healing superhydrophobicity, *J. Phys. Chem. C*, 2015, **119**(13), 7109–7114.

71 J. Yang, H. Xu, L. Zhang, Y. Zhong, X. Sui and Z. Mao, Lasting superhydrophobicity and antibacterial activity of Cu nanoparticles immobilized on the surface of dopamine modified cotton fabrics, *Surf. Coat. Technol.*, 2017, **309**, 149–154.

72 F. Guo, Q. Wen, Y. Peng and Z. Guo, Simple one-pot approach toward robust and boiling-water resistant superhydrophobic cotton fabric and the application in oil/water separation, *J. Mater. Chem. A*, 2017, **5**(41), 21866–21874.

73 H. Wang, H. Zhou, S. Liu, H. Shao, S. Fu, G. C. Rutledge, *et al.*, Durable, self-healing, superhydrophobic fabrics from fluorine-free, waterborne, polydopamine/alkyl silane coatings, *RSC Adv.*, 2017, **7**(54), 33986–33993.

74 Y. Luo, S. Wang, X. Fu, X. Du, H. Wang, M. Zhou, *et al.*, Fabrication of a Bio-Based Superhydrophobic and Flame-Retardant Cotton Fabric for Oil–Water Separation, *Macromol. Mater. Eng.*, 2021, **306**(3), 1–12.

75 S. Lu, Y. Zhao, X. Hu, Y. Lin and Y. Ke, Biomimetic fabrication of micron/nano-meter assembled superhydrophobic polymer fiber fabrics for oil/water separation, *Mater. Lett.*, 2020, **262**, 127152.

76 X. Yan, X. Zhu, Y. Ruan, T. Xing, G. Chen and C. Zhou, Biomimetic, dopamine-modified superhydrophobic cotton fabric for oil–water separation, *Cellulose*, 2020, **27**(13), 7873–7885.

77 Q. Zeng, P. Ma, X. Su, D. Lai, X. Lai, X. Zeng, *et al.*, Facile fabrication of superhydrophobic and magnetic poly(lactic acid) nonwoven fabric for oil–water separation, *Ind. Eng. Chem. Res.*, 2020, **59**(19), 9127–9135.

78 L. Chen and Z. Guo, A facile method to mussel-inspired superhydrophobic thiol-textiles@polydopamine for oil–water separation, *Colloids Surf. A*, 2018, **554**, 253–260.

79 B. Wang, L. Xing, T. Xing and G. Chen, Preparation of Stable POSS-Based Superhydrophobic Textiles Using Thiol-Ene Click Chemistry, *Polymers*, 2022, **14**(7), 1426.

80 Z. Xu, K. Miyazaki and T. Hori, Fabrication of polydopamine-coated superhydrophobic fabrics for oil–water separation and self-cleaning, *Appl. Surf. Sci.*, 2016, **370**, 243–251.

81 J. Zhang, L. Zhang and X. Gong, Design and fabrication of polydopamine based superhydrophobic fabrics for efficient oil–water separation, *Soft Matter*, 2021, **17**(27), 6542–6551.

82 X. Yu, X. Shi, F. Xue, W. Bai, Y. Li, Y. Liu, *et al.*, SiO<sub>2</sub> nanoparticle-containing superhydrophobic materials with enhanced durability *via* facile and scalable spray method, *Colloids Surf. A*, 2021, **626**, 127014.

83 A. S. Belal, M. M. A. Khalil, M. Soliman and S. Ebrahim, Novel superhydrophobic surface of cotton fabrics for removing oil or organic solvents from contaminated water, *Cellulose*, 2020, **27**(13), 7703–7719.

84 D. Cheng, Y. Zhang, X. Bai, Y. Liu, Z. Deng, J. Wu, *et al.*, Mussel-inspired fabrication of superhydrophobic cotton fabric for oil/water separation and visible light photocatalytic, *Cellulose*, 2020, **27**(9), 5421–5433.

85 X. Dong, S. Gao, J. Huang, S. Li, T. Zhu, Y. Cheng, *et al.*, A self-roughened and biodegradable superhydrophobic coating with UV shielding, solar-induced self-healing and versatile oil–water separation ability, *J. Mater. Chem. A*, 2019, **7**(5), 2122–2128.

86 R. Su, L. Li, J. Kang, X. Ma, D. Chen, X. Fan, *et al.*, AgNPs-thiols modified PVDF electrospun nanofiber membrane with a highly rough and pH-responsive surface for controllable oil/water separation, *J. Environ. Chem. Eng.*, 2022, **10**, 108235.

87 S. Zhu, T. Lu, Z. Wang, D. Peng, L. Wang and Y. Huang, Durable superhydrophobic PDA-ZIF-8/PDMS composite fabric with photothermal antibacterial and self-cleaning properties, *Mater. Lett.*, 2024, **360**, 6–10.

88 C. Long, X. Long, Y. Cai, X. Wang, C. Li, Y. Qing and Y. Zhao, Long-lived nanoparticle-embedded superhydrophobic membranes with rapid photocatalytic properties and continuous oil – water separation, *Chem. Eng. J.*, 2024, **482**, 148743.

89 M. Hatami, S. Panahi, M. Moezzi, F. Barez and Y. w. Chang, Novel eco-friendly bio-nano-hybridized woolen felts for effective oil/water separation, *J. Environ. Chem. Eng.*, 2024, **12**, 111614.

90 S. Li, J. h. Lin, H. t. Ren, B. c. Shiu and F. Sun, Photothermal-driven pH-responsive fiber composite membrane for oil-wastewater purification, *J. Environ. Chem. Eng.*, 2024, **12**, 111757.

91 H. Zhang and Z. Guo, Robust self-healing superhydrophobic cotton fabric for durable and efficient oil–water separation, *New J. Chem.*, 2023, **47**(40), 18769–18778.

92 B. Wang, L. Xing, T. Xing and G. Chen, Preparation of Superhydrophobic Fabric Based on Dopamine and Michael Addition under Ultraviolet Light, *ACS omega*, 2023, **8**(49), 46786–46793.

93 M. Wang, M. Peng, J. Zhu, Y. D. Li and J. B. Zeng, Mussel-inspired chitosan modified superhydrophilic and underwater superoleophobic cotton fabric for efficient oil–water separation, *Carbohydr. Polym.*, 2020, **244**, 116449.

94 R. Liu, Q. Chen, M. Cao, J. Lin, F. Lin, W. Ye, *et al.*, Robust bio-inspired superhydrophilic and underwater superoleophobic membranes for simultaneously fast water and oil recovery, *J. Membr. Sci.*, 2021, **623**, 119041, DOI: [10.1016/j.memsci.2020.119041](https://doi.org/10.1016/j.memsci.2020.119041).



95 X. Zhong and Z. Guo, Simple and ultrahigh efficient superhydrophilic polydopamine-coated  $\text{TiO}_2$  cotton for oil-water separation, *J. Bionic Eng.*, 2023, **20**(3), 900–909.

96 G. Zhang, Y. Zhan, S. He, L. Zhang, G. Zeng and Y. H. Chiao, Construction of superhydrophilic/underwater superoleophobic polydopamine-modified h-BN/poly(arylene ether nitrile) composite membrane for stable oil-water emulsions separation, *Polym. Adv. Technol.*, 2020, **31**(5), 1007–1018.

97 X. Huang, S. Zhang, W. Xiao, J. Luo, B. Li, L. Wang, *et al.*, Flexible PDA@ACNTs decorated polymer nanofiber composite with superhydrophilicity and underwater superoleophobicity for efficient separation of oil-in-water emulsion, *J. Membr. Sci.*, 2020, **614**, 118500.

98 H. Zhao, Y. He, Z. Wang, Y. Zhao and L. Sun, Mussel-inspired fabrication of pda@pan electrospun nanofibrous membrane for oil-in-water emulsion separation, *Nanomaterials*, 2021, **11**(12), 1–15.

99 N. Liu, X. Li, J. Li, Y. Cao and L. Feng, Hierarchical architectures of Ag clusters deposited biomimetic membrane: Synthesis, emulsion separation, catalytic and antibacterial performance, *Sep. Purif. Technol.*, 2020, **241**, 116733.

100 J. Wang, Z. Yu, X. Xiao, Z. Chen, G. Zeng, Y. Liu and J. Hou, In situ grown, super-hydrophilic and multifunctional hydroxyapatite composite membrane for oil-water separation, *Sep. Purif. Technol.*, 2024, **329**, 125088.

101 Y. Cui, X. Zheng, T. Xu, B. Ji, J. Mei and Z. Li, Underwater Super-Oleophobic Composite Membrane for Efficient Oil – Water Separation, *Molecules*, 2023, **28**(8), 3396.

102 D. D. Hu, Y. D. Li, Y. Weng, H. Q. Peng and J. B. Zeng, Mussel inspired stable underwater superoleophobic cotton fabric combined with carbon nanotubes for efficient oil/water separation and dye adsorption, *Appl. Surf. Sci.*, 2023, **631**, 157566.

103 X. Li, Y. Chen, Y. Chen, D. Chen, Q. Wang and Y. Wang, J. Zhou,  $\text{SiO}_2$  modified superwetting cotton fabric with anti-crude oil fouling, mechanical stability and corrosion resistance, *J. Environ. Chem. Eng.*, 2023, **11**, 109540.

104 Y. Xin, B. Qi, X. Wu, C. Yang and B. Li, Different types of membrane materials for oil-water separation: Status and challenges, *Colloid Interface Sci. Commun.*, 2024, **59**, 100772.

105 H. Zhang, F. Wang and Z. Guo, The antifouling mechanism and application of bio-inspired superwetting surfaces with effective antifouling performance, *Adv. Colloid Interface Sci.*, 2024, **325**, 103097.

106 L. Mohapatra and S. H. Yoo, Superwetting materials as catalysts in photocatalysis: State-of-the-Art review, *Chem. Eng. J.*, 2024, **481**, 148537.

107 H. Jiang, R. Luo, Y. Li and W. Chen, Recent advances in solid–liquid–gas three-phase interfaces in electrocatalysis for energy conversion and storage, *EcoMat*, 2022, **4**(4), e12199.

108 S. Barthwal, S. Uniyal and S. Barthwal, Nature-Inspired Superhydrophobic Coating Materials: Drawing Inspiration from Nature for Enhanced Functionality, *Micromachines*, 2024, **15**(3), 391.

109 T. P. Rasitha, N. G. Krishna, B. Anandkumar, S. C. Vanithakumari and J. Philip, A comprehensive review on anticorrosive/antifouling superhydrophobic coatings: Fabrication, assessment, applications, challenges and future perspectives, *Adv. Colloid Interface Sci.*, 2024, 103090.

110 M. S. Bell and A. Borhan, A Volume-Corrected Wenzel Model, *ACS Omega*, 2020, **5**(15), 8875–8884.

111 X. Mao, Y. Wang, X. Yan, Z. Huang, Z. Gao, Y. Wang, *et al.*, A review of superwetting membranes and nanofibers for efficient oil/water separation, *J. Mater. Sci.*, 2023, **58**, 3–33.

112 H. Lee, S. M. Dellatore, W. M. Miller and P. B. Messersmith, Mussel-Inspired Surface Chemistry for Multifunctional Coatings, *Science*, 2007, **318**(5849), 426–430.

113 C. Qi, L. H. Fu, H. Xu, T. F. Wang, J. Lin and P. Huang, Melanin/polydopamine-based nanomaterials for biomedical applications, *Sci. China:Chem.*, 2019, **62**, 162–188.

114 J. Yong, Q. Yang, X. Hou and F. Chen, Relationship and Interconversion Between Superhydrophilicity, Underwater Superoleophilicity, Underwater Superaerophilicity, Superhydrophobicity, Underwater Superoleophobicity, and Underwater Superaerophobicity: A Mini-Review, *Front. Chem.*, 2020, **8**, 828.

115 M. Wang, D. D. Hu, Y. D. Li, H. Q. Peng and J. B. Zeng, Biobased mussel-inspired underwater superoleophobic chitosan derived complex hydrogel coated cotton fabric for oil/water separation, *Int. J. Biol. Macromol.*, 2022, **209**, 279–289.

116 P. Yang, J. Yang, Z. Wu, X. Zhang, Y. Liu and M. Lu, Facile fabrication of superhydrophilic and underwater superoleophobic surfaces on cotton fabrics for effective oil/water separation with excellent anti-contamination ability, *Colloids Surf. A*, 2021, **628**, 127290.

117 M. Zhang, D. Liang, W. Jiang and J. Shi, Ag@ $\text{TiO}_2$  NPs/PU composite fabric with special wettability for separating various water-oil emulsions, *RSC Adv.*, 2020, **10**(58), 35341–35348.

118 D. D. Hu, Y. D. Li, Y. Weng, H. Q. Peng and J. B. Zeng, Fabrication of sustainable and durable superwetting cotton fabrics with plant polyphenol for on-demand oil/water separation, *Ind. Crops Prod.*, 2022, **186**, 115264.

119 X. Li, Y. Chen, Y. Chen, D. Chen, Q. Wang and Y. Wang, Superhydrophilic and Underwater Superoleophobic Cotton Fabric for Oil–Water Separation and Removal of Heavy-Metal Ion, *ACS Omega*, 2022, 30184–30196, DOI: [10.1021/acsomega.2c03298](https://doi.org/10.1021/acsomega.2c03298).

120 X. Li, Y. Chen, Y. Chen, D. Chen, Q. Wang and Y. Wang, Superhydrophilic and Underwater Superoleophobic Cotton Fabric for Oil–Water Separation and Removal of Heavy-Metal Ion, *ACS Omega*, 2022, 30184–30196, DOI: [10.1021/acsomega.2c03298](https://doi.org/10.1021/acsomega.2c03298).

121 H. Zhao, Y. He, Z. Wang, Y. Zhao and L. Sun, Mussel-Inspired Fabrication of PDA@PAN Electrospun Nanofibrous Membrane for Oil-in-Water Emulsion



Separation, *Nanomaterials*, 2021, 3434, DOI: [10.3390/nano11123434](https://doi.org/10.3390/nano11123434).

122 X. Huang, S. Zhang, W. Xiao, J. Luo, B. Li, L. Wang, *et al.*, Flexible PDA@ACNTs decorated polymer nanofiber composite with superhydrophilicity and underwater superoleophobicity for efficient separation of oil-in-water emulsion, *J. Membr. Sci.*, 2020, **614**, 118500.

123 G. Zhang, Y. Zhan, S. He, L. Zhang, G. Zeng and Y. H. Chiao, Construction of superhydrophilic/underwater superoleophobic polydopamine-modified h-BN/poly(arylene ether nitrile) composite membrane for stable oil-water emulsions separation, *Polym. Adv. Technol.*, 2020, **31**(5), 1007–1018.

124 C. Chen, D. Weng, A. Mahmood, S. Chen and J. Wang, Separation Mechanism and Construction of Surfaces with Special Wettability for Oil/Water Separation, *ACS Appl. Mater. Interfaces*, 2019, **11**(11), 11006–11027.

125 C. Chen, R. Jiang and Z. Guo, Bionic functional membranes for separation of oil-in-water emulsions, *Friction*, 2024, **12**(9), 1909–1928.

126 C. Chen, L. Chen, D. Weng, S. Chen, J. Liu and J. Wang, Revealing the mechanism of superwetting fibrous membranes for separating surfactant-free water-in-oil emulsions, *Sep. Purif. Technol.*, 2022, **288**, 120621.

127 C. Chen, L. Chen, S. Chen, Y. Yu, D. Weng, A. Mahmood, *et al.*, Preparation of underwater superoleophobic membranes via TiO<sub>2</sub> electrostatic self-assembly for separation of stratified oil/water mixtures and emulsions, *J. Membr. Sci.*, 2020, **602**, 117976.

128 N. Zhang, X. Yang, Y. Wang, Y. Qi, Y. Zhang, J. Luo, *et al.*, A review on oil/water emulsion separation membrane material, *J. Environ. Chem. Eng.*, 2022, **10**(2), 107257.

129 Y. Deng, M. Dai, Y. Wu and C. Peng, Emulsion system, demulsification and membrane technology in oil-water emulsion separation: A comprehensive review, *Crit. Rev. Environ. Sci. Technol.*, 2023, **53**(12), 1254–1278.

130 R. S. Sutar, X. Wu, S. S. Latthe, B. Shi, R. Xing and S. Liu, Efficient separation of oil-water emulsions: Competent design of superwetting materials for practical applications, *J. Environ. Chem. Eng.*, 2023, 111299.

131 X. Cheng, T. Li, L. Yan, Y. Jiao, Y. Zhang, K. Wang, *et al.*, Biodegradable electrospinning superhydrophilic nanofiber membranes for ultrafast oil-water separation, *Sci. Adv.*, 2023, **9**(34), eadh8195.

132 N. Y. Abu-Thabit, A. K. Azad, K. Mezghani, S. Akhtar, A. S. Hakeem, Q. A. Drmosh, *et al.*, Rapid, Sustainable, and Versatile Strategy Towards Fabricating Superhydrophobic Cotton Textile Membranes for Separation of Emulsified and Stratified Oil/Water Mixtures, *Sep. Purif. Technol.*, 2024, **330**, 125352.

133 Z. Yang, Q. Liu, J. Li, Y. Dong and X. Y. Yang, Janus superwetting fabric for effective emulsion separation, *Chem. Lett.*, 2024, **53**(1), upad007.

134 R. Hu, J. Yang, S. Li, T. Zhang, H. Xiao, Y. Liu, *et al.*, Fabrication of special wettability functionalized Mg(OH)<sub>2</sub>@cotton fabric for oil/water mixtures and emulsions separation, *Cellulose*, 2020, **27**(13), 7739–7749.

135 Z. Wang, Y. Wang and G. Liu, Rapid and efficient separation of oil from oil-in-water emulsions using a Janus cotton fabric, *Angew. Chem.*, 2016, **128**(4), 1313–1316.

136 Y. Li, Z. Feng, Y. He, Y. Fan, J. Ma and X. Yin, Facile way in fabricating a cotton fabric membrane for switchable oil/water separation and water purification, *Appl. Surf. Sci.*, 2018, **441**, 500–507. Available from: <https://www.sciencedirect.com/science/article/pii/S0169433218304057>.

137 G. Miao, F. Li, Z. Gao, T. Xu, X. Miao, G. Ren, *et al.*, Ag/polydopamine-coated textile for enhanced liquid/liquid mixtures separation and dye removal, *iScience*, 2022, **25**(5), 104213.

138 Z. Jin, L. Yang, S. Shi, T. Wang, G. Duan, X. Liu, *et al.*, Flexible polydopamine bioelectronics, *Adv. Funct. Mater.*, 2021, **31**(30), 2103391.

139 H. Wang, H. Zhou, S. Liu, H. Shao, S. Fu, G. C. Rutledge, *et al.*, Durable, self-healing, superhydrophobic fabrics from fluorine-free, waterborne, polydopamine/alkyl silane coatings, *RSC Adv.*, 2017, **7**(54), 33986–33993.

140 C. Zhang, Y. Ou, W. Lei, L. Wan, J. Ji and Z. Xu, CuSO<sub>4</sub>/H<sub>2</sub>O<sub>2</sub>-induced rapid deposition of polydopamine coatings with high uniformity and enhanced stability, *Angew. Chem., Int. Ed.*, 2016, **55**(9), 3054–3057.

141 X. Zhu, B. Yan, X. Yan, T. Wei, H. Yao, M. S. Mia, *et al.*, Fabrication of non-iridescent structural color on silk surface by rapid polymerization of dopamine, *Prog. Org. Coat.*, 2020, **149**, 105904.

142 H. Yan, J. Zhen and Y. Yao, Fe 3+ and H 2 O 2 assisted dopamine rapid polymerization on melamine foam to activate PMS for organic pollutant degradation, *Environ. Sci.*, 2024, **10**(11), 2698–2708.

143 X. Zhou, S. Gao, D. Huang, Z. Lu, Y. Guan, L. Zou, *et al.*, Bioinspired, ultra-fast polymerization of dopamine under mild conditions, *Macromol. Rapid Commun.*, 2022, **43**(23), 2200581.

144 L. Tan, T. Zhu, Y. Huang, H. Yuan, L. Shi, Z. Zhu, *et al.*, Ozone-Induced Rapid and Green Synthesis of Polydopamine Coatings with High Uniformity and Enhanced Stability, *Adv. Sci.*, 2024, **11**(10), 2308153.

145 W. Zhang, Z. Liao, X. Meng, A. E. A. Niwaer, H. Wang, X. Li, *et al.*, Fast coating of hydrophobic upconversion nanoparticles by NaIO<sub>4</sub>-induced polymerization of dopamine: Positively charged surfaces and *in situ* deposition of Au nanoparticles, *Appl. Surf. Sci.*, 2020, **527**, 146821.

146 E. Eze, A. M. Omer, A. H. Hassanin, A. S. Eltaweil and M. E. El-Khouly, Cellulose acetate nanofiber modified with polydopamine polymerized MOFs for efficient removal of noxious organic dyes, *Environ. Sci. Pollut. Res.*, 2024, **31**(20), 29992–30008.

147 Z. Changani, A. Razmjou, A. Taheri-Kafrani, M. E. Warkiani and M. Asadnia, Surface modification of polypropylene membrane for the removal of iodine using polydopamine chemistry, *Chemosphere*, 2020, **249**, 126079.



148 X. Zhu, Z. Gao, F. Li, G. Miao, T. Xu, X. Miao, *et al.*, Superlyophobic graphene oxide/polydopamine coating under liquid system for liquid/liquid separation, dye removal, and anti-corrosion, *Carbon*, 2022, **190**, 329–336.

149 J. Li, S. Yuan, J. Zhu and B. Van der Bruggen, High-flux, antibacterial composite membranes *via* polydopamine-assisted PEI-TiO<sub>2</sub>/Ag modification for dye removal, *Chem. Eng. J.*, 2019, **373**, 275–284.

150 F. f. Ma, D. Zhang, N. Zhang, T. Huang and Y. Wang, Polydopamine-assisted deposition of polypyrrole on electrospun poly (vinylidene fluoride) nanofibers for bidirectional removal of cation and anion dyes, *Chem. Eng. J.*, 2018, **354**, 432–444.

151 A. Telli and M. Taş, In-situ functionalization of cotton fabrics with polydopamine and silver nanoparticles for multifunctional applications, *Cellulose*, 2024, 1–15.

152 R. Chen, B. Lin and R. Luo, Recent progress in polydopamine-based composites for the adsorption and degradation of industrial wastewater treatment, *Heliyon*, 2022, **8**(12), e12105.

